Planta (2022) 255:77
https://doi.org/10.1007/s00425-022-03857-8

ORIGINAL ARTICLE

Metabolome of *Ceratodon purpureus* (Hedw.) Brid., a cosmopolitan moss: the influence of seasonality

Wilton R. Sala-Carvalho[1] · Francisco P. Montessi-Amaral[1] · Marisia P. Esposito[1] · Richard Campestrini[1] · Magdalena Rossi[1] · Denilson F. Peralta[2] · Claudia M. Furlan[1]

Received: 4 January 2022 / Accepted: 10 February 2022

Abstract

Main conclusion ***Ceratodon purpureus*** **showed changes in disaccharides, flavonoids, and carotenoids throughout annual seasons. These changes indicate harsher environmental conditions during the dry period, directing metabolic precursors to enhance the antioxidant system.**

Abstract Bryophytes are a group of land plants comprising mosses (Bryophyta), liverworts (Marchantyophyta), and hornworts (Antocerotophyta). This study uses the molecular networking approach to investigate the influence of seasonality (dry and rainy seasons) on the metabolome and redox status of the moss *Ceratodon purpureus* (Hedw.) Brid., from Campos do Jordão, Brazil. Samples of *C. purpureus* were submitted to three extraction methods: 80% methanol producing the soluble fraction (intracellular compounds), followed by debris hydrolysis using sodium hydroxide producing the insoluble fraction (cell wall conjugated compounds), both analyzed by HPLC–MS; and extraction using pre-cooled methanol, separated into polar and non-polar fractions, being both analyzed by GC–MS. All fractions were processed using the Global Natural Product Social Molecular Network (GNPS). The redox status was assessed by the analysis of four enzyme activities combined with the analysis of the contents of ascorbate, glutathione, carotenoids, reactive oxygen species (ROS), and malondialdehyde acid (MDA). During the dry period, there was an increase of most biflavonoids, as well as phospholipids, disaccharides, long-chain fatty acids, carotenoids, antioxidant enzymes, ROS, and MDA. Results indicate that *C. purpureus* is under harsher environmental conditions during the dry period, mainly due to low temperature and less water availability (low rainfall).

Keywords Abiotic factors · Bryophytes · Ecometabolomic · Flavonoids · Lipids · Sugars

Abbreviations

AsA	Ascorbate
APX	Ascorbate peroxidase
CAT	Catalase
DHA	Dehydroascorbate
GNPS	Global natural product social molecular network
GR	Glutathione reductase
GS	Glutathione
GSSG	Oxidized glutathione
LPC	Lysophosphatidylcholine
LPE	Lysophosphatidylethanolamine
LRI	Linear retention index
MDA	Malondialdehyde acid
MS^2	Tandem mass spectrometry
ROS	Reactive oxygen species
SOD	Superoxide dismutase

Communicated by Dorothea Bartels.

✉ Claudia M. Furlan
furlancm@ib.usp.br

Wilton R. Sala-Carvalho
wiltonsala@usp.br

[1] Department of Botany, Institute of Biosciences, University of São Paulo, Rua Do Matão, 277, SP 05508-090, Brazil

[2] Instituto de Pesquisas Ambientais, Avenida Miguel Estéfano, 3687, SP 04301-012, Brazil

Introduction

Bryophytes, a land plant group that comprises mosses (Bryophyta), liverworts (Marchantyophyta), and hornworts (Antocerotophyta), have remarkable ecological importance, constituting a major part of biodiversity in rainforests, marshes, mountains, and tundra. In arctic regions,

Published online: 03 March 2022

they are important in maintaining permafrost, as carbon pools, and in general, they contribute to water retention as an important component of Earth biogeochemical cycles. They are also colonizers of newly exposed environments, soil stabilizers, and humus accumulators (Hallingbäck and Hodgetts 2000).

This group of land plants presents distinct and shared characteristics, such as the similarity between ancient fossils and modern species, a haploid-dominant life cycle (gametophyte), water-dependence for sexual reproduction, and slower rates of molecular evolution when compared to angiosperms. Furthermore, colonization and diversification of land plants would have required major metabolic adaptations resulting in the production of substances serving as ultraviolet screens, antioxidants, and precursors for structural biopolymers to resist desiccation, but also allowing gas exchange (Renault et al. 2017). As avascular plants, bryophytes have evolved a unique diversity of bioactive compounds as part of their survival strategy.

In the last decade, studies regarding the Bryophyte genome, transcriptome, and metabolome were published. The main species studied were the liverwort *Marchantia polymorpha* L. (Bowman et al. 2017) and the mosses *Physcomitrella patens* (Hedw.) Bruch and Schimp. (Erxleben et al. 2012), *Pohlia nutans* (Li et al. 2019), and *Ceratodon purpureus* (Hedw.) Brid. (McDaniel et al. 2016; Carey et al. 2020). These studies bring attention to these bryophyte species being a particularly strong choice for combining preview knowledge of metabolomic and physiological studies to the relatively new research discipline of ecometabolomics, which combines metabolomic techniques with ecological studies to characterize the biochemical interactions of organisms across spatial and temporal variations (Peters et al. 2018).

In this sense, *Ceratodon purpureus* is a cosmopolitan moss species, present in a wide geographic range from polar to tropical areas (Biersma et al. 2020), and is also naturally found in Brazilian territory, but only at high-altitude Ombrophyllous forests, being mainly found in southeast Brazil (Sulamita et al. 2021). This species was reported as highly resilient, occurring in Antarctica extreme cold environment and in Australia hot deserts (Waterman et al. 2017), suggesting that these places submit species to similar stressful conditions (i.e. high solar radiation, contrasting temperatures, and water availability) requiring the triggering of similar chemical adaptations.

To address ecometabolomics on bryophytes, this study uses the molecular networking approach to investigate the influence of seasonality on the metabolome of a high-altitude Ombrophyllous forest Brazilian population of *C. purpureus*. Thus, this study aimed to assess *C. purpureus* metabolome and redox status in its natural Brazilian habitat during two periods of seasonality: the dry and the rainy season. Our results showed a variation in lipid, sugar, and phenolic metabolism throughout seasonality.

Materials and methods

Plant materials and sampling

Five samples of *Ceratodon purpureus* (Hedw.) Brid. were collected from Parque Estadual Campos do Jordão, São Paulo, Brazil (22°42′10"S, 45°28′16"W) at 1930 m.a.s.l.), in August 2018 (dry season) and January 2019 (rainy season) (authorizations: SISGEN AA37B2E; SISBIO 70,893-1). As a small size species, to obtain enough moss mass for chemical analyses, the five samples were composed of multiple individuals, representing cluster samples. As a dioecious species, samples were also composed of a mix of both female and male individuals, but only the gametophytes were used for chemical investigation. *C. purpureus* occurs as cushions growing on the soil and all material was collected by removing a substantial part of the soil before cleaning at the laboratory facility. The fresh material was mechanically thoroughly sorted to remove the soil part and the sporophytes; gametophyte aliquots were stored at − 80 °C before extractions. For both seasons, a small part of the samples was freeze-dried to transform the results to a dry mass unity. Sampling was performed under stable weather conditions with sunshine at least 1 day before sampling and during sampling. Sampling was conducted between 10:00 and 11:00 am. Voucher specimens are stored in the SP Herbarium.

Monthly data of temperature, rainfall, and air humidity were obtained from the Meteorological Station in Campos do Jordão through the National Institute of Meteorology (INMET). For this meteorological station, solar radiation was not available. The data were used to construct a climate diagram for each year of plant collection.

HPLC-MS^2 analysis

For HPLC-tandem mass (MS^2) analysis, 150 mg of plant material was macerated with 15 mL of 80% methanol for 24 h. The supernatant was collected corresponding to the intracellular extract. The residue of the maceration was incubated (twice) at room temperature in sodium chloride (NaCl) solution (1 M, 7.5 mL) for 15 min each, methanol (7.5 mL), and then with methanol-chloroform (1:1, v/v, 7.5 mL), and finally washed with methanol (7.5 mL) for 15 min. After each incubation, the supernatants were discarded (modified from Waterman et al. 2017). The residue was dried and submitted to alkaline hydrolysis using sodium hydroxide (NaOH) (1 M, 7.5 mL) for 24 h. The supernatant was collected, acidified to pH 3 using hydrochloric acid (HCl), and submitted to solid phase extraction (SPE). The

SPE Strata C18-E column (Phenomenex) was activated and equilibrated using methanol and ultrapure water, respectively. The extract was loaded into the column and eluted with 6 mL of the following solvents: ultrapure water, followed by 5% methanol, and then methanol. The methanol fraction was collected to compose the cell wall extract. Both the soluble fraction (intracellular compounds) and the insoluble fraction (cell wall conjugated compounds) were dried, weighted, and solubilized in methanol for HPLC-MS^2 analyses. Samples were injected into HPLC (CBM-20A, Shimadzu) coupled to mass spectrometry (Amazon Speed ETD, Bruker) equipped with the Agilent Eclipse Plus C18 column (150 × 4.6 mm, 3.5 µm) at 40 °C. A volume of 3 µL of the extract was injected using the mobile phase acetonitrile (A) and ultrapure acidified water (B), initiating with 10% of A (0–6 min), increasing to 15% (6–7 min), maintaining isocratic for 15 min, increasing to 50% (22–32 min), increasing to 100% (32–42 min), and keeping isocratic for 8 min. The solvent flow was 1.0 mL min^{-1}. Metabolites were electron spray ionized in positive mode and detected using multiple reaction monitoring modes.

HPLC-MS^2 data treatment

The conversion of HPLC-MS^2 mass spectrum to mzML used ProteoWizzard (Kessner et al. 2008). The data treatment (deconvolution and peak alignment) was made using mzMine 2.53, with soluble and insoluble extracts analyzed together. The mass detection was made using centroid mode, considering the noise of all the ions with intensity below 1000 in the MS^1 level, and below 100 in the MS^2 level. The chromatogram was built using the Automated Data Analysis Pipeline (ADAP) module considering the presence of two points above the noise level to be considered a peak (Min group size in # of scans), the minimum highest intensity to be considered a peak in the chromatogram, and the group intensity threshold was of 3000 with an m/z tolerance of 0.5. The deconvolution steps were made using baseline cut-off with an m/z range of 0.5 Da and a retention time range of 0.5 min. Possible isotopes were grouped according to an m/z tolerance of 0.5 and retention time of 0.5 min, with a maximum charge of 2. The features alignment between the two samples analyzed was made using an m/z tolerance of 0.5, with a weight of 25% for m/z and 75% for retention time, and a tolerance of 0.5 min. The gap-filling between the samples was made using an intensity tolerance of 10%, an m/z tolerance of 0.5, and a retention time tolerance of 0.5 min. A file with the fragmentation of all the compounds was detected together with a peak area table. The results obtained with mzMine 2.53 were submitted to dereplication steps using Feature-Based Molecular Networking (FBMS) in the Global Natural product Social Molecular Network (GNPS) platform as the main database (http://gnps.uscd.edu), together with Reaxys (http://www.reaxys.com), SciFinder (http://scifinder.cas.org), NuBBEDB (http://nubbe.iq.unesp.br) as other options of database to dereplication. As a result, a matrix containing peak areas, molecular ions, retention times, and possible annotation of each compound, was generated. A molecular network was created using an online workflow in GNPS (Wang et al. 2016) and Cytoscape software to handle the molecular network. The data were clustered according to its MS^2, considering a parental mass of tolerance and a fragment of MS^2 of tolerance to create a consensus spectrum. The library search and the molecular network were conducted and constructed using a cosine score above 0.70 to be considered of a similar mass fragmentation spectrum.

The Metabolomics Standard Initiative (MSI), along with other scientific communities, has issued a guide to standardize the level of metabolite identity based on four criteria: Level 1, when a metabolite determined by manual inspection, software or web service is compared with an authentic standard under the same experimental condition; Level 2, occurs in the absence of an authentic sample; Level 3 is when only the metabolite class is determined; Level 4 is a completely unknown metabolite (Valli et al. 2019).

It was considered as annotated (Level 2) the compounds that GNPS suggested with a cosine score above 0.70 and with a difference below 1.5 amu between the molecular ion of the extract substance and the possible GNPS library identification. If the cosine score was above 0.70 but the difference between the molecular ion of the extract substance and the possible GNPS library identification was above 1.5 amu, it was considered of the same class of the suggestion and the cluster that it belongs to (Level 3). Therefore, the suggestion was made by analyzing the fragmentation spectrum and with library and database search comparison (MSI Levels 2 and 3).

GC–MS analysis

For GC–MS analysis, 50 mg of material were crushed and extracted with 700 µL of pre-cooled methanol (− 20 °C). Together with the extractive solvent were added 60 µL of adonitol (0.2 mg mL^{-1}, as an internal standard for polar phase) and 2.5 µL of tridecanoic acid (0.2 mg mL^{-1}, as an internal standard for non-polar phase). The mixture was incubated for 10 min at 70 °C and 950 rpm and centrifuged for 10 min at 11,000 g. The supernatant was transferred to new tubes and 375 µL of chloroform and 750 µL of ultrapure water were added (both pre-cooled). The mixture was shaken and centrifuged for 15 min at 2200 g, with the polar and non-polar phases being collected separately.

The polar phase was derivatized using methoxyamine hydrochloride (28 µL, for two hours at 37 °C) and 48 µL of N-Methyl-N-(trimethylsilyl)trifluoroacetamide (MSTFA) for 30 min at 37 °C. Samples were injected (1 µL) into

gas chromatography (6850 Network GC System, Agilent) coupled to mass spectrometry (5975C VL MSD, Agilent) (GC–MS) equipped with the Agilent VF-5MS column (30 m, 250 µm, 0.25 µm) and a pre-column (10 m, 0.25 mm). The initial column temperature was adjusted to 70 °C for 5 min, increasing at a rate of 5 °C min^{-1} to a final temperature of 295 °C, with a total run time of 50 min. Helium was the carrier gas at 1 mL min^{-1}. Injection temperature was 230 °C, ion source 200 °C, and quadrupole 150 °C; with electron impact ionization of 70 eV, working in the full-scan acquisition mode ranging between 50 and 600 m/z at 2.66 scan s^{-1}. The non-polar phase was derivatized with 50 µL pyridine and 50 µL of N,O-bis-(trimethylsilyl)-trifluoroacetamide (BSTFA) for 1 h at 70 °C. Samples were injected (1 µL) into the same GC–MS equipped with an Agilent HP5-MS capillary column (30 m, 250 µm, 0.25 µm). An initial column temperature was adjusted to 100 °C for 5 min, and increased at a rate of 5 °C min^{-1} to a final temperature of 320 °C, with a total run time of 49 min. Helium was the carrier gas at 1 mL min^{-1}; injection temperature 300 °C, ion source 230 °C, and quadrupole 150 °C; electron impact ionization of 70 eV, working in the full-scan acquisition mode ranging between 50 and 600 m/z at 2.66 scan s^{-1}.

GC–MS data treatment

Polar and non-polar phases were analyzed separately. Mass spectrum data treatment of each set (deconvolution, peak alignment, and Linear Retention Index (LRI) calculated through a C_8 to C_{40} alkane standard) together with the compound identification and dereplication was made using GNPS generating a feature table with the peak area, molecular ion, retention time and possible identification of each compound. A minimum cosine Index of 0.67 was applied and a LRI window of 30 was set to identify compounds. Compounds with a cosine Index above the minimum but with no LRI match were considered of the same class from the suggestion given by the GNPS. The LRI of identified compounds was compared to three databases: Golm Metabolome Database (GMD: http://gmd.mpimp-golm.mpg.de), MassBank Europe (https://massbank.eu/MassBank/), and National Institute of Standards and Technology (NIST: https://webbook.nist.gov). The molecular network was created with the Library Search/Molecular Network GC workflow at GNPS (Wang et al. 2016) and was manipulated using Cytoscape. The precursor ion mass tolerance was set to 2000 Da. The cosine score was set above 0.7 and a minimum of 6 matched peaks to consider a relationship between the nodes. The connection between the nodes was only kept between the 10 most similar nodes, with the maximum size of a molecular family of 100. The library spectra were filtered in the same manner.

Enzymes and protein determination

For all enzymatic extractions and protein determination, 250 mg of plant material were homogenized in an extraction buffer solution containing potassium phosphate buffer (50 mM pH 7.8), 5 mM ascorbic acid, 5 mM ethylenediamine tetra-acetic acid (EDTA), and 5 mM dithiothreitol (DTT). Each sample was centrifuged with 1.5 mL of the extraction buffer and 30 mg of polyvinylpolypyrrolidone (PVPP) at 10,000 g (4 °C) for 10 min (modified from Domingos et al. 2015).

Catalase (CAT) activity was determined at 25 °C using 16 µL of plant extract in 174 µL of potassium phosphate buffer (100 mM pH 7.5). A 200 nM hydrogen peroxide (H_2O_2) solution was prepared immediately before use and 10 µL were dispensed in each well by the microplate reader Synergy H1 (Biotek). The activity was determined following the decomposition of H_2O_2 for 2 min, by decreasing the absorbance at 240 nm.

Glutathione reductase (GR) activity was measured in a reaction mixture containing 3 µL of leaf extract, 140 µL of potassium phosphate buffer (100 mM pH 7.5), 71 µL of 1 mM 2'-nitrobenzoic acid 5,5'-dithiobis (DTNB), and 14 µL of 0.1 mM NADPH. The reaction was monitored at 412 nm for 3 min at 30 °C after the addition of 14 µL of 1 mM oxidized glutathione (GSSG) directly dispensed in each well by the microplate reader. The reaction was initiated by the addition of NADPH, which allows the reduction of GSSG by the enzyme GR.

Ascorbate peroxidase (APX) activity was determined using a reaction solution consisting of potassium phosphate buffer (100 mM pH 7.0) and 1 mM EDTA. For each sample, 20 µL of the plant extract, 150 µL of the reaction solution, and 20 µL of 5 mM ascorbic acid were mixed. The reaction was monitored at 290 nm for 3 min at 30 °C by the decomposition of H_2O_2 after the addition of 10 µL of 200 nM H_2O_2 directly dispensed in each well by the microplate reader.

Superoxide dismutase (SOD) activity was measured in a reaction mixture containing 40 µL of nitro blue tetrazolium (NBT), 40 µL of methionine, 40 µL of EDTA, 80 µL of potassium phosphate buffer (100 mM pH 7.0), 16 µL of riboflavin, and 16 µL of plant extract. After 30 min of exposure to fluorescent light (80 W), the absorbance of the mixture was measured at 560 nm. The controls for each sample were protected from light. The enzyme activity was determined by inhibiting the reduction of NBT, by enzymatic dismutation of the superoxide.

Protein was determined using the Bradford reagent (Sigma-Aldrich). For each sample, 20 µL of the diluted Bradford reagent (4:1) and 40 µL of the plant extract were mixed and analyzed at 590 nm. Bovine serum albumin (BSA; 500 µg mL^{-1}) was used as standard curves.

Non-enzymatic compounds determination

Ascorbate (AsA) and glutathione (GSH) in reduced (AsA; GSH), oxidized (DHA, GSSG) and total (AsA + DHA, GSG + GSSG) were obtained by HPLC at 245 and 194 nm, respectively. The extraction was carried out from 150 mg of plant material in an extraction buffer composed of 6% metaphosphoric acid (HPO_3) and 1 mM EDTA. After centrifugation at 10,000 g and to determine the reduced forms, 100 µL of the extract were diluted in 400 µL of the mobile phase (orthophosphoric acid pH 2.3, H_3PO_4). Samples (20 µL) were injected into HPLC (Agilent 1260) equipped with the Agilent Eclipse Zorbax Eclipse XDB-C18 (150 × 4.6 mm; 5 µm). For the analysis of the total contents, 20 µL of 0.4% DTT diluted in sodium phosphate buffer (0.2 M pH 7.0) and 10 µL of 45% dipotassium phosphate (K_2HPO_4) were added to the same amount of extract (100 µL), remaining in the dark for 20 min and interrupting the reaction with 20 µL of 2 M H_3PO_4, then adding 350 µL of water (Alves et al. 2020).

Carotenoid and chlorophyll contents were obtained from 200 mg of plant material adding 100 µL of saturated NaCl, 200 µL of dichloromethane, and 500 µL of extraction solution (hexane:ethyl ether 1:1, v/v). The extraction took place in an ultrasonic bath for 5 min and was then centrifuged at 13,000 g at 4 °C for 5 min to recover the upper organic phase. The procedure was repeated for another 4 × and the final volume was collected and vacuum dried. After solubilizing with 300 µL of ethyl acetate, extracts were analyzed by HPLC (Agilent 1260) equipped with the Phenomenex Luna C18 (250 × 4.6 mm; 5 µm); mobile phase: acetonitrile:water (9:1, v/v) and ethyl acetate. Detection was achieved at 450 nm (neoxanthin, violaxanthin, lutein, β-carotene, lycopene, and chlorophyll b), 650 nm (chlorophyll a), 286 nm (phytoene), and 347 nm (phytofluene) (Lira et al. 2017).

Reactive oxygen species and malondialdehyde determination

Hydrogen peroxide (H_2O_2) contents were determined by samples homogenization with trichloroacetic acid (TCA). The reaction mixture consisted of supernatant extract, potassium phosphate buffer (100 mM, pH 7.0), and potassium iodide reagent (KI). The reaction was developed for 1 h in darkness and absorbance was measured at 390 nm (modified from Esposito et al. 2018).

Hydroxyl radical ($^{\bullet}OH$) concentrations were estimated using 2-deoxyribose oxidative degradation. The principle of the assay is the quantification of the 2-deoxyribose degradation product, MDA, by its condensation with thiobarbituric acid (TBA). The absorbance of solutions was measured at 532 nm (modified from Esposito et al. 2018).

Superoxide ($O_2^{\bullet-}$) production rate was determined using the hydroxylamine oxidation method. Samples were homogenized and the supernatant was mixed with potassium phosphate buffer (pH 7.8) and hydroxylamine chloride. p-Aminobenzene sulfonic acid, α-naphthylamine, and n-butyl alcohol were added and the final supernatant was used for measuring absorbance at 530 nm (modified from Esposito et al. 2018).

Malondialdehyde (MDA) contents were determined in homogenized plant material in trichloroacetic acid and then trichloroacetic acid containing thiobarbituric acid was added to the supernatant, which was maintained for 30 min at 95 °C in a water bath. The samples were then rapidly cooled on ice. The absorbance was measured at 535 and 600 nm to determine the MDA content (modified from Esposito et al. 2018).

Data analysis

Significant differences between the dry and the rainy seasons relative to biochemical responses–concentration of non-enzymatic and enzymatic antioxidants, chlorophylls, carotenoids, reactive oxygen species, and malondialdehyde–were determined by one-way ANOVA using the Sigma Stat 11.0 software. When necessary, the data were transformed to reach normal distribution and equal variances. The Holm-Sidak method was employed as a post hoc test to identify significant differences between seasons.

For chemical composition (GC and HPLC results) was used R software (version 3.6.3) for one-way ANOVA. For the non-normal distributed data was used Kruskal–Wallis post hoc test, and the Student's *t* test was used for the parametric data.

Principal Component Analysis (PCA) was performed using Fitopac (version 2.1) (Shepherd 2010) to compare and identify chemical profiles from groups of samples from each season of collection.

Results

Meteorological conditions in Campos do Jordão

Monthly data of temperature, rainfall, and air humidity obtained from the Meteorological Station in Campos do Jordão were used to create two climate diagrams, one for each year of plant collection (Fig. 1a). Samples of *C. purpureus* were collected in August (2018), at the end of the dry season, which comprises the months of April–September. During this period (April to September 2018), the total precipitation was 135.2 mm, with a mean humidity of 83% and a mean daily temperature of 12.9 °C (daily maxima/minima of 24.2/ − 0.6 °C). The species was also collected in February (2019), in the middle of the rainy season, which

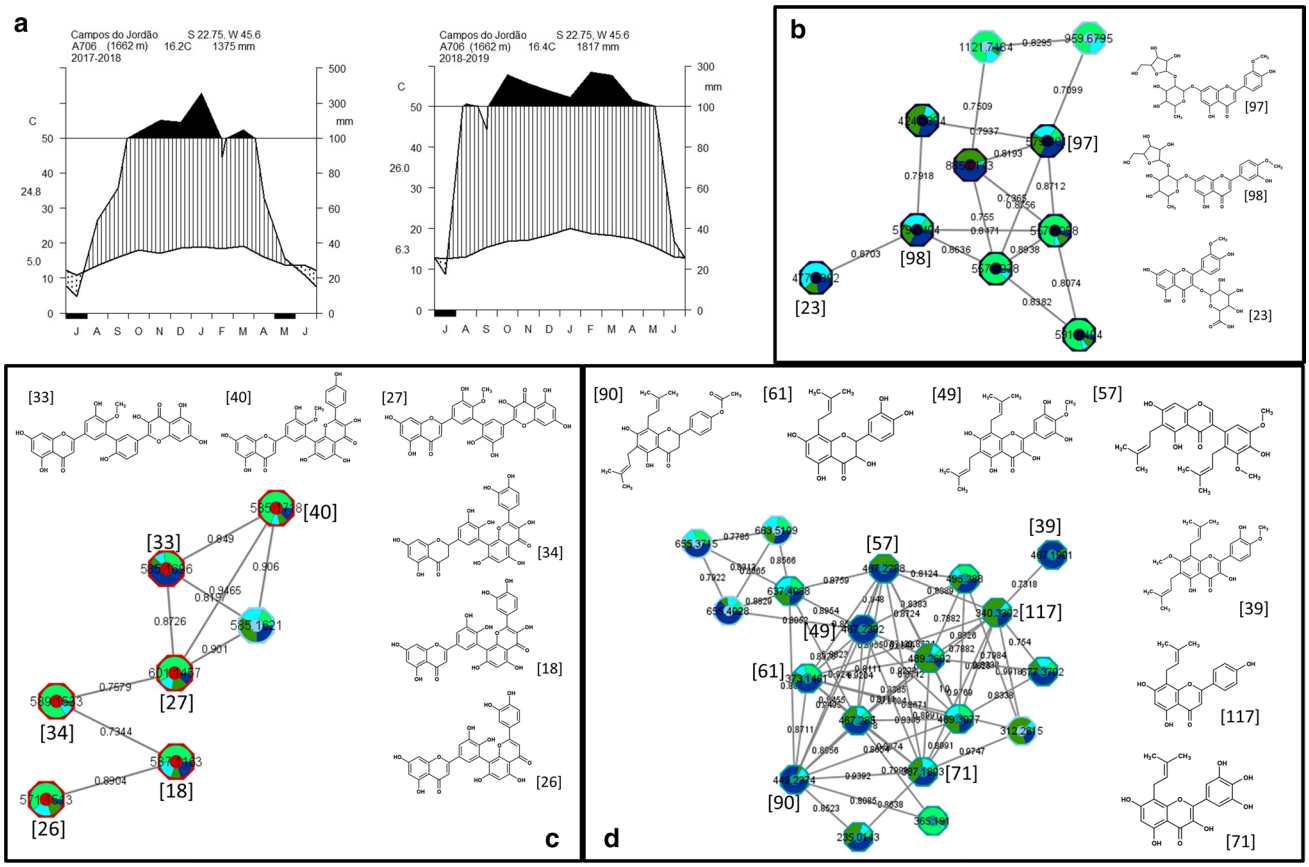

Fig. 1 Selected clusters from the molecular network of *Ceratodon purpureus:* **a** Climate diagrams for Campos do Jordão during 2018 and 2019 (plant collection: dry season, August 2018; rainy season, February 2019). **b** Glycosylated flavonoid. **c** Biflavonoids. **d** Prenylated flavonoids. Each node is proportionally colored with the abundance of each compound observed for rainy (blue) and dry (green) seasons, and their abundances in each cell compartment, intracellular extract (light colors) and cell wall extract (dark colors). Possible molecular structures are represented for the compound's annotation (numbers are associated to Tables 1, 2)

comprises the months of October–May. During the rainy season (October 2019 to May 2019), the total precipitation was 798.4 mm, with the mean relative humidity of 88% and the mean daily temperature of 17 ºC (daily maxima/minima of 28.2/4.6 °C).

Ecometabolomics of *Ceratodon purpureus*

GNPS platform allowed clustering compounds according to their MS spectra (LC-MS^2) into six major classes: flavonoids (biflavonoids; prenylated and glycosylated flavonoids); glycerol esters of fatty acids; phospholipids [lysophosphatidylcholine (LPC) and lysophosphatidylethanolamine (LPE)]; fatty acids derivatives (oxo fatty acids and hydroxylated fatty acids); diglycerides; and peptides. Annotation of these compounds followed four approaches: GNPS suggestions, the mass difference between the linked nodes, literature data, and other MS databases (Supplementary Table S1).

One of the major clusters grouped seven biflavonoids (Fig. 1c). The node 571 m/z, breaks into 419 m/z, and this loss of 152 amu corresponds to cleavage in the C-ring, also originating the 445 m/z fragment and a loss of 126 amu (another break of the C-ring), suggesting luteolin-(5'→8″)-luteolin [26]. Connected to [26] (cosine score 0.89) there is a node of 587 m/z and this difference of 16 amu from [26] corresponds to a gain of a hydroxyl group in one of the luteolin fragments, suggesting this compound as luteolin-(5'→8″)-quercetin [18]. Connected to [18] (cosine score 0.79), there is a node of 589 m/z, and this difference of 2 amu suggests a loss of the double ligand in the C-ring of one of the fragments, therefore, since its similarity is higher to [18], the compound was annotated as eriodictyol-(5'→8″)-quercetin [34]. Connected to [34], there is a node of 601 m/z (cosine score 0.75), this increase of 12 amu is probably due to methylation in one of the hydroxyl groups together with a double ligand in the C-ring of eriodictyol, suggesting this compound as diosmetin-(5'→8‴)-quercetin [27]. The node of 585 m/z connected to [27] (cosine score 0.94) shows a loss of 16 amu, probably due to a loss of a hydroxyl group in the quercetin moiety, therefore, the

compound was annotated as diosmetin-(5'→8″)-kaempferol [40]. Also connected to [27] (cosine score 0.83), there is another node of 585 m/z and this compound was annotated as diosmetin-(5'→5‴)-kaempferol [33]. Furthermore, the biflavonoid annotated as luteolin-(5'→8″)-apigenin [44] (555 m/z) was also detected in *C. purpureus*.

Biflavonoids found in *C. purpureus* were majorly found in the intracellular extract, as [18], [26], [34], and [40], but [33] was majorly found at the cell wall extract. Regarding the dry and rainy seasons, there was a distinguished high abundance of [18], [26], [34], and [40] during the dry season, while [33] and the unidentified biflavonoid seem to accumulate during the rainy season. Specifically in the rainy season [26] and [34] tend to be more abundant intracellularly than at the cell wall while [18] cell wall abundance seems to be higher in the rainy season than in the dry season. Apart from biflavonoids being majorly found intracellularly, they were statistically more abundant in the cell wall extract during the dry season compared to the rainy season, including Luteolin-(5'→8")-apigenin (Fig. 1; Tables 1, 2).

Another cluster grouped prenylated flavonoids (Fig. 1d). The 449 m/z node (cosine score: 0.80) breaks into 393 m/z and 337 m/z, both losses of 56 amu corresponding to cleavage of prenyl groups, annotating 6,8-diprenylapigenin-4'-*O*-acetate [90]. Connected to [90], there are two nodes of 467 m/z (cosine score 0.92 and 0,95) and this gain of 18 amu might be due to the presence of an additional hydroxyl group in these structures, together with the loss of the double ligand in the C-ring, annotating these two compounds as pumilaisoflavone C [57] and 6,8-diprenylmearnsetin [49]. Connected to [49], the 387 m/z node (cosine score 0.95) lacks 80 amu, which corresponds to the absence of one of the prenyl groups together with the loss of a methyl group in mearnsetin, therefore this compound was annotated as 8-prenylmyricetin [71]. Also connected to [49], there are two other compounds, 8-prenyltaxifolin [61] (cosine score 0.88), and 8-prenylapigenin [117] (cosine score 0.97). Connected to [117], the 467 m/z node (cosine score 0.73) annotates 8-prenylutilinol [39]. All of these prenylated flavonoids were majorly found conjugated to the cell wall, as [39] and [49], and frequently more abundant in the rainy season. Only [117] showed high contents in the dry season, while [57] and [71] were similarly abundant among the seasons. When present intracellularly the prenylated flavonoids are usually more abundant in the rainy season, [71] and [90], or similarly, [117], compared to the dry season, apart from [61] which showed high abundance in the dry season. Even though the prenylated flavonoid abundance was not statistically different between the seasons, that was relevant for some specific compounds as prenylutilinol, more abundant in the cell wall extract during the rainy season, and 8-prenyltaxifolin, more abundant intracellularly in the dry season (Fig. 1; Tables 1, 2).

Another cluster revealed the presence of glycosylated flavonoids (Fig. 1b). The 579 m/z node breaks into 301 m/z losing 278 amu, due to a loss of a pentose/arabinose moiety, this compound was annotated as chrysoeriol-7-*O*-xyloside arabinofuranoside [98]. Connected to [98] the 477 m/z node (cosine score 0.87) breaks in the major fragment of 301 m/z, losing 176 amu, annotating this compound as chrysoeriol-3-*O*-glucuronic acid [23]. Also, in this cluster, there is another 579 m/z node with a similar fragmentation pattern, suggesting diosmetin 7-*O*-glucopyranosyl-4'-*O*-rhamnopyranoside [97].

There is also a cluster composed of flavonoids with a hexose moiety. This annotation was based on the loss of 162 amu, correspondent to a hexose, suggesting 3 compounds: padmakastin [15] (449 m/z), astragalin [20] (449 m/z), and isorhamnetin-3-galactoside [22] (479 m/z). Also, there is a 536 m/z node that breaks in the major fragment of 287 m/*z* and this loss of 248 amu might be related to a malonyl-hexoside moiety, suggesting 6″-*O*-malonylpadmakastin [4].

The distribution of these glycosidic flavonoids was similar in proportion between the cell wall and the cytoplasm, except for [20] and [22], almost exclusive conjugated to the cell wall; [47] and [4] were detected majorly conjugated to the cell wall, while [15] was observed majorly in the intracellular extract. The same was observed regarding seasonality, in the intracellular extract, there was a significantly higher abundance of compounds [20], [22], and [23] during the rainy season, while [47] had a higher abundance during the dry season. Statistically, glycosylated flavonoids were more abundant in the rainy season than in the dry season at the intracellular level, especially for apigenin diglycoside. Even though those abundance variations were noticed in the main flavonoid groups, the total abundance of flavonoids was not statistically relevant among the seasons, in both cellular extracts. (Tables 1, 2).

Two other large cluster of *C. purpureus* molecular network grouped the phospholipids (LPC and LPE). These two classes of compounds, as well as the phospholipid class itself, showed higher abundance during the dry period at intracellular level (Tables 1, 2). Analyzing the mass fragmentation patterns of these compounds, it was possible to observe a cluster composed by LPC 18:4/0:0 (516 m/z) [64], LPC 18:3/0:0 (518 m/z) [73], LPC 20:5/0:0 (542 m/z) [74], LPC 20:4/0:0 (544 m/z) [86], two isomers of LPC 18:2/0:0 (520 m/z) [87] and [88], and LPC 18:1/0:0 (522 m/z) [99]. For LPE' cluster, the mass fragmentation patterns suggested LPE 18:3/0:0 (476 m/z) [68], LPE 20:4/0:0 (500 m/z) [70], LPE 16:1/0:0 (452 m/z) [72], LPE 18:2/0:0 (478 m/z) [78], LPE 20:3/0:0 (502 m/z) [79], LPE 16:0/0:0 (454 m/z) [89], and LPE 18:1/0:0 (480 m/z) [92] (Supplementary Table S1).

The polar phase analyzed by GC–MS detected 56 compounds grouped into six major classes: sugars (mono, di,

Table 1 Peak area of hydroethanol intracellular extract detected by HPLC-MS^2 in gametophyte of *Ceratodon purpureus* from Campos do Jordão collected during the rainy and the dry seasons.

Nº	RT[a] (min)	Possible annotation	Rainy	Dry
		Total flavonoids	2.31E + 09 ± 1.53E + 09 a	3.38E + 09 ± 1,29E + 09 a
		Biflavonoid	1.71E + 09 ± 1.42E + 09 a	2.87E + 09 ± 1.19E + 09 a
18	18.33	Luteolin-(5'→8")-quercetin*	5.44E + 05 ± 6.27E + 06 a	1.41E + 06 ± 2.14E + 07 a
26	26.12	Luteolin-(5'→8")-luteolin*	1.30E + 06 ± 1.41E + 07 a	4.05E + 07 ± 5.26E + 07 a
27	28.61	Diosmetin-(5'→5"')-quercetin	2.70E + 06 ± 2.29E + 06 a	1.58E + 07 ± 1.29E + 07 a
33	29.62	Diosmetin-(5'→5"')-kaempferol	9.58E + 06 ± 1.12E + 07 a	2.40E + 07 ± 1.99E + 07 a
34	**29.64**	**Eriodictyol-(5'→8")-quercetin**	**7.10E + 07 ± 7.74E + 07 b**	**6.08E + 08 ± 4.45E + 08 a**
37	30.60	Diosmetin-(5'→8")-quercetin*	2.74E + 07 ± 4.18E + 07 a	3.96E + 06 ± 2.37E + 06 a
40	30.78	Diosmetin-(5'→8")-kaempferol	8.61E + 06 ± 8.38E + 06 a	6.90E + 07 ± 5.31E + 07 a
44	31.50	Luteolin-(5'→8")-apigenin	1.58E + 09 ± 1.26E + 09 a	2.10E + 09 ± 7.65E + 08 a
		Prenylated flavonoid	2.05E + 08 ± 8.28E + 07 a	2.75E + 08 ± 1.24E + 08 a
39	30.71	Prenylutilinol	1.24E + 06 ± 7.87E + 05 a	2.00E + 06 ± 8.37E + 05 a
49	32.71	6,8-Diprenylmearnsetin	1.82E + 06 ± 1.07E + 06 a	4.44E + 06 ± 3.07E + 06 a
50	**32.76**	**6-Prenyl-7-Hydroxyisoflavanone**	**3.82E + 06 ± 2.98E + 06 b**	**5.53E + 07 ± 4.08E + 07 a**
52	33.14	8-Prenyl-7-Hydroxyisoflavanone	3.42E + 07 ± 1.75E + 07 a	3.55E + 07 ± 3.02E + 07 a
57	33.97	Pumilaisoflavone C	2.04E + 06 ± 1.12E + 06 a	2.74E + 06 ± 8.41E + 05 a
61	**34.93**	**8-Prenyltaxifolin**	**5.59E + 06 ± 2.71E + 06 b**	**1.15E + 07 ± 3.26E + 06 a**
67	35.72	8-Prenylquercetin	6.66E + 07 ± 2.79E + 07 a	4.99E + 07 ± 9.37E + 06 a
71	36.03	8-Prenylmyricetin	6.54E + 06 ± 5.09E + 06 a	3.52E + 06 ± 1.29E + 06 a
75	**36.53**	**8-Prenyl-7-Hydroxyflavanone**	**1.12E + 07 ± 9.42E + 06 b**	**7.48E + 07 ± 4.70E + 07 a**
81	**37.09**	**Bidwillon A**	**4.67E + 07 ± 2.53E + 07 a**	**1.54E + 07 ± 6.10E + 06 b**
90	38.16	6,8-Diprenylapigenin-4'-*O*-acetate*	1.13E + 07 ± 1.45E + 07 a	5.89E + 06 ± 3.56E + 06 a
93	38.38	6,8-Diprenylgenistein-4'-*O*-acetate*	8.55E + 06 ± 1.05E + 07 a	1.01E + 07 ± 9.90E + 06 a
117	46.5	8-Prenylapigenin*	5.02E + 06 ± 5.82E + 06 a	4.16E + 06 ± 2.12E + 06 a
		Glycosilated flavonoid	**3.65E + 08 ± 7.71E + 07 a**	**2.08E + 08 ± 6.15E + 07 b**
4	2.00	6"-*O*-Malonylpadmakastin	2.24E + 06 ± 1.01E + 06 a	3.12E + 06 ± 1.56E + 06 a
8	3.03	Luteolin-4'-glucoside	7.40E + 05 ± 3.10E + 05 a	6.23E + 05 ± 1.88E + 05 a
13	9.16	Naringenin-6,8-di-*C*-glucoside*	8.95E + 05 ± 8.13E + 05 a	1.20E + 06 ± 1.54E + 06 a
14	9.92	Lucenin 2	3.52E + 05 ± 2.07E + 05 a	3.30E + 05 ± 1.18E + 05 a
15	11.02	Padmakastin*	7.77E + 05 ± 7.93E + 05 a	4.40E + 06 ± 8.41E + 06 a
16	12.74	Vitexin -4"-O-glucoside	2.75E + 05 ± 1.28E + 05 a	1.98E + 05 ± 4.83E + 04 a
17	16.27	Luteolin-7-neohesperidoside 4-D-glucoside*	3.24E + 06 ± 5.42E + 06 a	4.56E + 06 ± 3.28E + 06 a
20	22.14	Astragalin	2.08E + 05 ± 1.44E + 05 a	1.33E + 05 ± 3.45E + 04 a
21	24.42	Apigenin 4'-*O*-glucoside*	7.58E + 06 ± 1.41E + 07 a	1.99E + 05 ± 4.20E + 04 a
22	25.08	Isorhamnetin 3-galactoside*	1.63E + 05 ± 1.13E + 05 a	1.47E + 05 ± 4.02E + 04 a
23	25.62	Chrysoeriol-3-*O*-glucoronic acid *	1.01E + 07 ± 1.97E + 07 a	3.64E + 05 ± 7.47E + 04 a
24	25.96	Diosmin*	2.46E + 06 ± 4.05E + 06 a	4.23E + 06 ± 3.94E + 06 a
31	**29.53**	**Luteolin 7-glucuronide**	**1.61E + 06 ± 7.26E + 05 b**	**8.01E + 06 ± 5.30E + 06 a**
97	**39.49**	**Apigenin 7-*O*-α-D-glucopyranosyl-4'-*O*-α-L-rhamnopyranoside**	**1.18E + 08 ± 4.81E + 07 a**	**5.56E + 07 ± 3.18E + 07 b**
98	39.51	Chrysoeriol-7-*O*-xylosoide (1–2)-arabinofuranoside	2.17E + 08 ± 7.92E + 07 a	1.29E + 08 ± 3.45E + 07 a
113	45.99	Formononetin derivative	8.08E + 06 ± 5.66E + 06 a	1.26E + 07 ± 9.41E + 06 a
		Other flavonoids	2.27E + 07 ± 1.56E + 07 a	2.11E + 07 ± 7.78E + 06 a
25	**25.97**	**Gardenin**	**9.63E + 05 ± 8.29E + 05 b**	**5.55E + 06 ± 3.08E + 06 a**
36	30.08	Naringenin	6.77E + 05 ± 1.93E + 05 a	8.36E + 05 ± 3.41E + 05 a
58	33.98	Sakuranetin	1.39E + 07 ± 1.13E + 07 a	1.31E + 07 ± 7.17E + 06 a
125	**52.37**	**Luteolin acetate**	**7.16E + 06 ± 4.49E + 06 a**	**1.61E + 06 ± 7.60E + 05 b**
		Fatty acid ester	4.76E + 07 ± 3.09E + 07 a	1.66E + 07 ± 1.16E + 07 a
35	29.81	Linolenic acid, ethyl ester*	3.27E + 06 ± 3.79E + 06 a	8.44E + 06 ± 9.82E + 06 a
96	**39.27**	**Nonadecatrienoic acid, methyl ester**	**6.23E + 06 ± 3.46E + 06 a**	**1.93E + 06 ± 7.42E + 05 b**

Table 1 (continued)

Nº	RT[a] (min)	Possible annotation	Rainy	Dry
104	41.28	13,16-Docosadienoic acid, methyl ester	2.64E + 06 ± 2.82E + 07 a	3.11E + 06 ± 1.71E + 06 a
105	41.52	10,13-Nonadecadienoic acid, methyl ester*	1.17E + 07 ± 1.25E + 07 a	3.08E + 06 ± 1.22E + 06 a
		Peptide	**1.15E + 07 ± 7.01E + 06 b**	**8.70E + 07 ± 2.71E + 07 a**
3	1.99	Gamma-glutamyl valine	5.83E + 06 ± 4.35E + 06 a	8.94E + 06 ± 3.37E + 06 a
9	**3.28**	**Gamma-glutamylleucine**	**4.69E + 06 ± 2.58E + 06 b**	**5.67E + 07 ± 1.46E + 07 a**
11	**4.41**	**Gamma-glutamylphenylalanine**	**9.84E + 05 ± 6.48E + 05 b**	**2.13E + 07 ± 1.15E + 07 a**
12	9.02	Gln-Ile-Lys*	1.23E + 06 ± 1.63E + 07 a	3.11E + 06 ± 9.25E + 05 a
		Glycerides	1.03E + 09 ± 5.11E + 08 a	1.20E + 09 ± 2.14E + 08 a
47	32.23	Monogalactosylmonoacylglycerol	1.11E + 07 ± 1.31E + 07 a	4.16E + 06 ± 2.63E + 06 a
65	35.62	Monolinolenin (9c,12c,15c)	1.23E + 08 ± 8.93E + 07 a	1.42E + 08 ± 5.52E + 07 a
80	37.04	2-Eicosapentaenoyl glycerol	7.39E + 07 ± 7.12E + 07 a	1.46E + 07 ± 4.91E + 06 a
100	39.75	TG (13:0/16:0/18:0)	6.95E + 07 ± 3.11E + 07 a	4.53E + 07 ± 3.12E + 07 a
102	40.28	Monolinolenin	1.50E + 08 ± 1.04E + 08 a	8.35E + 07 ± 1.75E + 07 a
106	41.62	1-Linoleoylglycerol*	9.83E + 07 ± 6.54E + 07 a	4.80E + 07 ± 2.20E + 07 a
107	41.66	1-Arachidonoylglycerol*	1.48E + 08 ± 1.00E + 08 a	5.11E + 07 ± 4.17E + 07 a
109	42.32	1-Hexadecanoyl-sn-glycerol	2.68E + 07 ± 2.77E + 07 a	7.12E + 06 ± 2.19E + 06 a
110	42.63	Monoolein	4.24E + 07 ± 3.79E + 07 a	1.35E + 07 ± 7.39E + 06 a
115	**46.2**	**MGDG (16:2/18:3)**	**4.44E + 06 ± 1.38E + 06 a**	**2.86E + 06 ± 9.95E + 05 b**
116	**46.32**	**MGDG (18:3/18:3)**	**8.89E + 07 ± 2.36E + 07 b**	**2.95E + 08 ± 5.34E + 07 a**
118	49.17	DG (18:4/21:0)	3.71E + 06 ± 2.12E + 06 a	4.36E + 06 ± 2.65E + 06 a
119	49.31	DG (18:4/21:0)	2.76E + 06 ± 6.69E + 05 a	2.62E + 06 ± 7.33E + 05 a
120	50.03	DG (17:1/20:2)*	4.74E + 06 ± 5.05E + 06 a	2.13E + 06 ± 4.38E + 05 a
121	50.24	DG (19:0/20:4)	3.13E + 06 ± 1.41E + 06 a	2.03E + 06 ± 5.67E + 05 a
122	**50.5**	**MGDG (16:0/18:3)**	**1.31E + 08 ± 8.46E + 07 b**	**3.07E + 08 ± 1.06E + 08 a**
123	51.53	TG (18:1/18:1/18:0)*	3.09E + 06 ± 1.86E + 06 a	3.21E + 06 ± 2.46E + 06 a
124	51.78	DGDG (18:3/18:3)	1.25E + 07 ± 8.03E + 06 a	1.92E + 07 ± 1.94E + 07 a
		Lysophosphatidylcholine	**1.81E + 09 ± 9.54E + 08 b**	**1.59E + 10 ± 2.43E + 09 a**
30	29.21	LPC (17:1)*	1.24E + 06 ± 4.70E + 05 a	3.17E + 06 ± 3.24E + 06 a
64	**35.55**	**LPC (18:4)**	**5.46E + 06 ± 5.06E + 06 b**	**1.21E + 08 ± 6.57E + 07 a**
73	**36.28**	**LPC (18:3)**	**1.40E + 08 ± 1.03E + 08 b**	**3.68E + 09 ± 9.57E + 08 a**
74	**36.33**	**LPC (20:5)**	**2.60E + 07 ± 2.32E + 07 b**	**1.15E + 09 ± 3.30E + 08 a**
76	36.61	LPC (16:0)*	5.01E + 07 ± 4.52E + 07 a	1.25E + 08 ± 8.29E + 07 a
86	**37.54**	**LPC (20:4)**	**1.38E + 08 ± 1.03E + 08 b**	**2.34E + 09 ± 4.87E + 08 a**
87	**37.56**	**LPC (18:2)***	**2.20E + 08 ± 1.53E + 08 b**	**3.15E + 09 ± 1.40E + 09 a**
88	**37.63**	**LPC (18:2)**	**3.94E + 08 ± 2.67E + 08 b**	**3.65E + 09 ± 6.55E + 08 a**
99	**39.70**	**LPC (18:1)**	**3.45E + 08 ± 2.58E + 08 b**	**1.17E + 09 ± 3.23E + 08 a**
101	40.14	LPC (20:3)	3.13E + 08 ± 9.74E + 07 a	3.11E + 08 ± 2.30E + 08 a
103	41.03	LPC (14:0)	1.74E + 08 ± 3.49E + 07 a	1.70E + 08 ± 3.03E + 07 a
		Lysophosphatidylethanolamine	**4.94E + 08 ± 2.02E + 08 b**	**1.18E + 09 ± 2.77E + 08 a**
68	**35.83**	**LPE (18:3)**	**7.64E + 06 ± 4.57E + 06 b**	**1.08E + 08 ± 2.57E + 07 a**
70	**35.98**	**LPE (20:5)**	**5.49E + 06 ± 3.83E + 06 b**	**1.41E + 08 ± 7.60E + 07 a**
72	**36.17**	**LPE (16:1)**	**1.82E + 07 ± 1.38E + 07 b**	**6.55E + 07 ± 3.32E + 07 a**
78	**37.01**	**LPE (18:2)***	**3.94E + 07 ± 5.42E + 07 b**	**1.78E + 08 ± 5.94E + 07 a**
79	**37.03**	**LPE (20:4)**	**4.71E + 07 ± 4.61E + 07 b**	**2.73E + 08 ± 5.53E + 07 a**
89	37.83	LPE (16:0)*	4.19E + 07 ± 3.49E + 07 a	8.91E + 07 ± 7.08E + 07 a
92	**38.35**	**LPE (18:1)**	**2.03E + 07 ± 1.35E + 07 b**	**7.62E + 07 ± 1.64E + 07 a**
108	41.81	LPE (18:0)	3.14E + 08 ± 4.20E + 07 a	2.50E + 08 ± 3.84E + 07 a
		Fatty acid derivatives	1.87E + 08 ± 6.06E + 07 a	1.82E + 08 ± 4.85E + 07 a
28	28.69	9,12-Hexadecadienoic acid, 6-hydroxy-	5.49E + 05 ± 1.66E + 05 a	9.47E + 05 ± 3.47E + 05 a
32	29.58	9-Tetracosenoic acid	1.73E + 06 ± 3.95E + 05 a	3.70E + 06 ± 2.86E + 06 a

Table 1 (continued)

Nº	RT[a] (min)	Possible annotation	Rainy	Dry
38	30.61	3,6-Pentadecadienedioic acid	1.06E + 06 ± 3.91E + 05 a	1.50E + 06 ± 4.21E + 05 a
41	30.80	15-Tetracosenoic acid*	1.96E + 06 ± 1.14E + 06 a	1.21E + 06 ± 3.56E + 05 a
42	31.15	9,10,12-Trihydroxyoctadecanoic acid	1.05E + 06 ± 2.51E + 05 a	1.25E + 06 ± 9.30E + 05 a
43	**31.23**	**Oxooleic acid**	**8.98E + 05 ± 2.38E + 05 b**	**4.53E + 06 ± 2.93E + 06 a**
45	**31.73**	**4,9,11-Pentadecatrienoic acid, 15-hydroxy-***	**7.25E + 05 ± 1.70E + 05 b**	**2.24E + 06 ± 2.36E + 06 a**
46	31.83	7-Hexadecenoic acid, 16-hydroxy-	1.86E + 06 ± 1.08E + 06 a	1.84E + 06 ± 8.26E + 05 a
48	32.46	4,9,11,13-Pentadecatetraenoic acid, 15-hydroxy-	1.32E + 06 ± 9.03E + 05 a	8.92E + 05 ± 1.98E + 05 a
51	33.02	Oleic acid	1.40E + 07 ± 6.32E + 06 a	1.01E + 07 ± 4.03E + 06 a
54	33.32	Eicosanolactone	8.84E + 07 ± 3.74E + 07 a	7.14E + 07 ± 2.00E + 07 a
55	33.38	Pentacosanoic acid	7.83E + 06 ± 6.09E + 06 a	5.95E + 06 ± 2.10E + 06 a
59	34.23	2-Nonadecylbutanedioic acid*	5.87E + 06 ± 6.36E + 06 a	1.33E + 07 ± 8.69E + 06 a
66	35.65	Pinolenic acid	4.01E + 07 ± 4.42E + 07 a	4.36E + 06 ± 1.03E + 06 a
82	**37.27**	**9S-Hydroxy-10E,12Z,15Z-octadecatrienoic acid**	**6.51E + 07 ± 2.36E + 07 a**	**4.24E + 06 ± 1.84E + 06 b**
84	**37.41**	**19-Hydroxynonadecanoic acid**	**1.25E + 07 ± 7.80E + 06 a**	**2.27E + 06 ± 9.86E + 05 b**
91	**38.23**	**Linolenic acid**	**2.96E + 07 ± 1.83E + 07 b**	**1.28E + 08 ± 4.06E + 07 a**
95	39.20	13S-Hydroxy-9Z,11E,15Z-octadecatrienoic acid	3.05E + 06 ± 1.14E + 06 a	3.01E + 06 ± 5.48E + 05 a
		Soluble sugar	1.15E + 09 ± 5.69E + 08 a	8.09E + 08 ± 7.64E + 07 a
1	1.47	Melezitose	1.13E + 09 ± 5.57E + 08 a	5.57E + 08 ± 1.21E + 08 a
2	**1.94**	**Galactopinitol A**	**2.24E + 07 ± 1.47E + 07 b**	**2.34E + 08 ± 4.81E + 07 a**
		Terpenoid		
69	**35.97**	**Strobilactona A***	**6.79E + 07 ± 1.90E + 07 a**	**4.86E + 07 ± 7.18E + 06 b**
		Nucleotide	**1.86E + 07 ± 8.61E + 06 b**	**4.01E + 07 ± 5.05E + 06 a**
5	**2.04**	**3'-Guanylic acid**	**6.81E + 06 ± 3.31E + 06 a**	**2.22E + 06 ± 8.33E + 05 b**
6	**2.08**	**Adenosine**	**2.34E + 06 ± 1.22E + 06 a**	**1.81E + 06 ± 6.09E + 05 b**
7	2.11	5'-Adenylic acid	6.48E + 06 ± 3.39E + 06 a	3.03E + 07 ± 4.57E + 06 a
10	**3.67**	**N6-Threonylcarbamoyladenosine**	**2.98E + 06 ± 2.14E + 06 b**	**5.82E + 06 ± 1.08E + 06 a**
		Phenolic	3.00E + 08 ± 1.52E + 08 a	4.17E + 08 ± 1.49E + 08 a
29	**29.12**	**Tephrosin**	**1.17E + 06 ± 9.22E + 05 b**	**6.83E + 06 ± 4.31E + 06 a**
60	34.28	Arachidin 3	1.83E + 06 ± 1.21E + 06 a	3.43E + 06 ± 1.50E + 06 a
62	34.97	[7-(3,4-dihydroxyphenyl)-1-(4-hydroxyphenyl)heptan-3-yl] acetate*	3.23E + 06 ± 1.18E + 06 a	2.63E + 06 ± 1.78E + 06 a
63	34.99	Cercosporin	3.23E + 07 ± 4.21E + 07 a	4.28E + 07 ± 2.72E + 07 a
77	36.72	3,3',4,5,5'-Pentamethoxystilbene	2.51E + 08 ± 1.30E + 08 a	2.16E + 08 ± 1.19E + 08 a
83	**37.38**	**Flavestin***	**6.40E + 06 ± 7.61E + 06 b**	**1.41E + 08 ± 7.28E + 07 a**
112	44.5	Dipetalolactone	3.94E + 06 ± 2.30E + 06 a	3.63E + 06 ± 2.34E + 06 a
		Nitrogen compounds	6.66E + 08 ± 2.69E + 08 a	8.76E + 08 ± 2.46E + 08 a
19	21.75	3-Pyridinecarboxylic acid, 1,6-dihydro-5-methoxy-6-oxo-	1.04E + 05 ± 2.41E + 04 a	7.94E + 04 ± 1.38E + 04 a
53	33.22	Phytosphingosine	4.78E + 07 ± 3.27E + 07 a	5.87E + 07 ± 2.26E + 07 a
56	33.78	CocamidopropylBetaine	2.10E + 06 ± 8.82E + 05 a	2.61E + 06 ± 8.69E + 05 a
85	37.48	Asperphenamate*	7.61E + 07 ± 1.03E + 08 a	4.81E + 07 ± 4.57E + 07 a
111	42.87	Pheophorbide	4.50E + 08 ± 3.29E + 08 a	6.95E + 08 ± 2.25E + 08 a
114	46.16	Docosenamide dimer	3.91E + 07 ± 1.64E + 07 a	1.55E + 08 ± 2.83E + 07 a
		Others		
94	39.05	Tris(2-butoxyethyl) phosphate	2.45E + 07 ± 4.65E + 06 a	2.10E + 07 ± 7.68E + 06 a

Different letters indicate significant differences between rainy and dry seasons ($P < 0.05$, $n = 5$) and are highlighted in bold

[a]*RT* retention time

*Compounds with non-normal distribution

Table 2 Peak area of hydroethanol cell wall extract detected by HPLC-MS^2 in gametophyte of *Ceratodon purpureus* from Campos do Jordão collected during the rainy and the dry seasons.

Nº	RT[a] (min)	Possible annotation	Rainy	Dry
		Total flavonoids	2.17E + 09 ± 1.04E + 09 a	1.38E + 09 ± 3.51E + 08 a
		Biflavonoid	1.62E + 08 ± 8.60E + 07 b	5.23E + 08 ± 2.95E + 08 a
18	18.33	Luteolin-(5'→8")-quercetin	5.65E + 06 ± 5.90E + 06 a	2.67E + 06 ± 2.18E + 06 a
26	26.12	Luteolin-(5'→8")-luteolin	3.84E + 06 ± 2.00E + 06 a	9.51E + 06 ± 4.59E + 06 a
27	28.61	Diosmetin-(5'→5"')-quercetin	1.16E + 07 ± 7.74E + 06 a	1.15E + 07 ± 5.91E + 06 a
33	29.62	Diosmetin-(5'→5"')-Kaempferol*	4.75E + 07 ± 7.22E + 07 a	6.60E + 06 ± 2.69E + 06 a
34	29.64	Eriodictyol-(5'→8")-quercetin*	1.38E + 07 ± 1.01E + 07 a	2.63E + 07 ± 3.61E + 07 a
37	30.60	Diosmetin-(5'→8")-quercetin	4.43E + 06 ± 2.46E + 06 a	1.02E + 07 ± 6.90E + 06 a
40	30.78	Diosmetin-(5'→8")-kaempferol	1.31E + 07 ± 1.02E + 07 a	8.31E + 06 ± 4.76E + 06 a
44	**31.50**	**Luteolin-(5'→8")-apigenin**	**6.21E + 07 ± 5.77E + 07 b**	**4.48E + 08 ± 3.08E + 08 a**
		Prenylated flavonoid	1.15E + 09 ± 9.49E + 08 a	2.87E + 08 ± 1.39E + 08 a
39	**30.71**	**Prenylutilinol**	**1.82E + 08 ± 1.45E + 08 a**	**1.32E + 07 ± 1.05E + 07 b**
49	32.71	6.8-Diprenylmearnsetin*	3.21E + 08 ± 5.38E + 08 a	2.43E + 07 ± 3.78E + 07 a
50	32.76	6-Prenyl-7-Hydroxyisoflavanone*	3.79E + 06 ± 3.50E + 06 a	3.69E + 07 ± 5.89E + 07 a
52	33.14	8-Prenyl-7-Hydroxyisoflavanone	1.59E + 06 ± 6.75E + 05 a	5.40E + 06 ± 3.56E + 06 a
57	33.97	Pumilaisoflavone C*	9.42E + 07 ± 1.80E + 08 a	7.27E + 07 ± 9.00E + 07 a
61	34.93	8-Prenyltaxifolin	1.79E + 07 ± 2.09E + 07 a	5.33E + 06 ± 3.22E + 06 a
67	35.72	8-Prenylquercetin	2.92E + 07 ± 3.31E + 07 a	3.64E + 07 ± 1.18E + 07 a
71	36.03	8-Prenylmyricetin	1.40E + 07 ± 1.27E + 07 a	1.39E + 06 ± 1.01E + 07 a
75	36.53	8-Prenyl-7-hydroxyflavanone	7.64E + 06 ± 9.70E + 06 a	3.22E + 06 ± 1.62E + 06 a
81	37.09	Bidwillon A	4.03E + 07 ± 2.28E + 07 a	2.08E + 07 ± 1.23E + 07 a
90	38.16	6,8-Diprenylapigenin-4'-*O*-acetate*	8.72E + 07 ± 1.39E + 08 a	4.41E + 06 ± 3.02E + 06 a
93	38.38	6,8-Diprenylgenistein-4'-*O*-acetate*	3.33E + 08 ± 3.07E + 08 a	9.28E + 06 ± 9.36E + 06 a
117	46.5	8-Prenylapigenin*	1.52E + 07 ± 1.15E + 07 a	4.10E + 07 ± 4.29E + 07 a
		Glycosilated flavonoid	8.27E + 08 ± 4.74E + 08 a	4.58E + 08 ± 1.35E + 08 a
4	2.00	6"-*O*-Malonylpadmakastin	7.70E + 06 ± 5.84E + 06 a	4.12E + 06 ± 2.85E + 06 a
8	3.03	Luteolin-4'-Glucoside*	7.94E + 06 ± 1.26E + 07 a	5.92E + 06 ± 8.87E + 06 a
13	9.16	Naringenin-6,8-di-*C*-glucoside	3.19E + 08 ± 3.44E + 08 a	5.41E + 07 ± 2.58E + 07 a
14	9.92	Lucenin 2	4.07E + 06 ± 3.24E + 06 a	1.10E + 07 ± 1.06E + 07 a
15	11.02	Padmakastin	2.75E + 06 ± 2.23E + 06 a	1.43E + 06 ± 3.17E + 05 a
16	12.74	Vitexin -4"-*O*-glucoside	3.07E + 06 ± 2.09E + 06 a	2.74E + 07 ± 1.60E + 07 a
17	16.27	Luteolin-7-neohesperidoside 4-D-glucoside	4.42E + 06 ± 4.04E + 06 a	1.05E + 07 ± 5.13E + 06 a
20	**22.14**	**Astragalin**	**2.44E + 07 ± 1.75E + 07 a**	**1.92E + 06 ± 9.93E + 05 b**
21	24.42	Apigenin 4'-*O*-glucoside*	1.35E + 07 ± 2.10E + 07 a	1.02E + 06 ± 3.76E + 05 a
22	25.08	Isorhamnetin 3-galactoside	2.12E + 07 ± 2.27E + 07 a	2.47E + 06 ± 1.93E + 06 a
23	25.62	Chrysoeriol-3-*O*-glucoronic acid	3.80E + 06 ± 4.24E + 06 a	2.61E + 06 ± 1.56E + 06 a
24	25.96	Diosmin*	2.05E + 07 ± 3.29E + 07 a	2.09E + 07 ± 2.76E + 07 a
31	29.53	Luteolin 7-glucuronide	2.99E + 06 ± 1.38E + 06 a	7.92E + 06 ± 5.95E + 06 a
97	39.49	Apigenin 7-*O*-α-D-glucopyranosyl-4'-*O*-α-L-rhamnopyranoside	1.31E + 08 ± 5.63E + 07 a	9.98E + 07 ± 4.53E + 07 a
98	39.51	Chrysoeriol-7-*O*-xylosoide (1–2)-arabinofuranoside	2.63E + 08 ± 4.66E + 07 a	2.15E + 08 ± 1.49E + 08 a
113	**45.99**	**Formononetin derivative**	**2.08E + 06 ± 5.54E + 05 b**	**9.01E + 07 ± 4.06E + 07 a**
		Other flavonoids	3.00E + 07 ± 2.31E + 07 a	1.08E + 08 ± 1.01E + 08 a
25	25.97	Gardenin	4.20E + 06 ± 3.19E + 06 a	9.68E + 07 ± 1.00E + 08 a
36	30.08	Naringenin	1.43E + 07 ± 1.50E + 07 a	7.34E + 06 ± 2.70E + 06 a
58	33.98	Sakuranetin	3.29E + 06 ± 2.24E + 06 a	2.32E + 06 ± 1.53E + 06 a
125	**52.37**	**Luteolin acetate**	**8.24E + 06 ± 4.83E + 06 a**	**1.93E + 06 ± 1.32E + 06 b**
		Fatty acid ester	1.87E + 07 ± 5.25E + 06 a	2.79E + 07 ± 1.90E + 07 a
35	29.81	Linolenic acid, ethyl ester*	9.28E + 06 ± 5.90E + 06 a	7.25E + 06 ± 9.49E + 06 a
96	39.27	Nonadecatrienoic acid, methyl ester	1.29E + 06 ± 6.47E + 05 a	1.61E + 06 ± 7.06E + 05 a

Table 2 (continued)

Nº	RT[a] (min)	Possible annotation	Rainy	Dry
104	41.28	13,16-Docosadienoic acid, methyl ester*	3.70E + 06 ± 2.39E + 06 a	1.58E + 07 ± 1.96E + 07 a
105	41.52	10,13-Nonadecadienoic acid, methyl ester	4.39E + 06 ± 2.54E + 06 a	3.23E + 06 ± 7.62E + 05 a
		Peptide	2.35E + 07 ± 2.13E + 07 a	2.75E + 06 ± 1.16E + 06 a
3	1.99	Gamma-glutamyl valine	7.37E + 05 ± 3.90E + 05 a	6.97E + 05 ± 2.16E + 05 a
9	3.28	Gamma-glutamylleucine	1.96E + 07 ± 1.75E + 07 a	1.32E + 06 ± 8.86E + 05 a
11	4.41	Gamma-Glutamylphenylalanine*	3.08E + 06 ± 4.04E + 06 a	7.30E + 05 ± 3.67E + 05 a
12	9.02	Gln-Ile-Lys	1.15E + 08 ± 1.05E + 08 a	2.22E + 07 ± 1.11E + 07 a
		Glycerides	1.05E + 09 ± 5.45E + 08 a	6.03E + 08 ± 2.82E + 08 a
47	**32.23**	**Monogalactosylmonoacylglycerol***	**3.88E + 06 ± 2.01E + 06 b**	**4.12E + 07 ± 5.87E + 07 a**
65	35.62	Monolinolenin (9c,12c,15c)	4.12E + 06 ± 2.67E + 06 a	3.37E + 06 ± 8.04E + 05 a
80	37.04	2-Eicosapentaenoyl glycerol	2.36E + 06 ± 1.74E + 06 a	8.15E + 06 ± 5.79E + 06 a
100	39.75	Triacylglycerol 13:0–16:0–18:0	8.30E + 08 ± 5.47E + 08 a	3.82E + 08 ± 2.78E + 08 a
102	40.28	Monolinolenin	1.43E + 07 ± 1.01E + 07 a	2.39E + 07 ± 7.84E + 06 a
106	41.62	1-Linoleoylglycerol	9.44E + 06 ± 3.40E + 06 a	1.09E + 07 ± 3.64E + 06 a
107	41.66	1-Arachidonoylglycerol	1.01E + 07 ± 4.42E + 06 a	8.29E + 06 ± 4.10E + 06 a
109	42.32	1-Hexadecanoyl-sn-glycerol*	2.95E + 06 ± 1.37E + 06 a	3.92E + 06 ± 1.42E + 06 a
110	42.63	Monoolein	3.41E + 06 ± 8.79E + 05 a	2.82E + 06 ± 2.09E + 06 a
115	46.2	MGDG (16:2/18:3)	2.72E + 08 ± 2.12E + 08 a	1.85E + 08 ± 1.24E + 08 a
116	46.32	MGDG (18:3/18:3)	2.87E + 06 ± 6.73E + 05 a	3.24E + 06 ± 1.62E + 06 a
118	49.17	DG (18:4/21:0)*	1.09E + 07 ± 1.63E + 07 a	4.60E + 06 ± 1.24E + 07 a
119	49.31	DG (18:4/21:0)	1.77E + 07 ± 1.03E + 07 a	1.03E + 07 ± 9.72E + 06 a
120	50.03	DG (17:1/20:2)*	2.39E + 07 ± 2.76E + 07 a	2.99E + 07 ± 1.58E + 07 a
121	50.24	DG (19:0/20:4)*	2.16E + 07 ± 2.76E + 07 a	1.25E + 07 ± 1.58E + 07 a
122	50.5	MGDG (16:0/18:3)	1.13E + 07 ± 1.49E + 07 a	4.25E + 06 ± 1.69E + 06 a
123	51.53	TG (18:1/18:1/18:0)	6.70E + 07 ± 5.94E + 07 a	4.79E + 07 ± 3.67E + 07 a
124	51.78	DGDG (18:3/18:3)	4.21E + 06 ± 1.95E + 06 a	2.52E + 06 ± 9.17E + 05 a
		Lysophosphatidylcholine	2.09E + 09 ± 1.43E + 09 a	1.60E + 09 ± 5.45E + 08 a
30	29.21	LPC (17:1)	1.26E + 08 ± 1.41E + 08 a	4.73E + 07 ± 5.17E + 07 a
64	35.55	LPC (18:4)	7.85E + 06 ± 6.40E + 06 a	6.02E + 06 ± 4.37E + 06 a
73	36.28	LPC (18:3)	4.57E + 06 ± 4.20E + 06 a	5.20E + 06 ± 1.65E + 06 a
74	36.33	LPC (20:5)	4.01E + 06 ± 3.45E + 06 a	6.93E + 06 ± 3.96E + 06 a
76	36.61	LPC (16:0)*	6.86E + 06 ± 9.36E + 06 a	8.08E + 06 ± 4.87E + 06 a
86	**37.54**	**LPC (20:4)**	**3.03E + 06 ± 1.11E + 06 b**	**2.71E + 07 ± 1.76E + 07 a**
87	37.56	LPC (18:2)*	6.92E + 06 ± 5.22E + 06 a	3.15E + 07 ± 4.59E + 07 a
88	37.63	LPC (18:2)	5.56E + 06 ± 5.02E + 06 a	6.68E + 07 ± 7.91E + 07 a
99	39.70	LPC (18:1)*	5.27E + 06 ± 2.07E + 06 a	2.41E + 07 ± 3.73E + 07 a
101	40.14	LPC (20:3)	1.92E + 09 ± 1.43E + 09 a	1.28E + 09 ± 5.98E + 08 a
103	41.03	LPC (14:0)	1.27E + 08 ± 5.70E + 07 a	1.45E + 08 ± 7.16E + 07 a
		Lysophosphatidylethanolamine	3.78E + 08 ± 1.81E + 08 a	3.53E + 08 ± 5.95E + 07 a
68	35.83	LPE (18:3)	4.41E + 06 ± 2.13E + 06 a	4.01E + 06 ± 1.64E + 06 a
70	35.98	LPE (20:5)*	3.92E + 06 ± 1.94E + 06 a	5.46E + 06 ± 4.04E + 06 a
72	36.17	LPE (16:1)*	1.17E + 07 ± 1.77E + 07 a	3.07E + 06 ± 1.73E + 06 a
78	37.01	LPE (18:2)*	2.39E + 06 ± 1.40E + 06 a	2.91E + 06 ± 1.84E + 06 a
79	37.03	LPE (20:4)	2.74E + 06 ± 8.86E + 05 a	4.94E + 06 ± 2.53E + 06 a
89	37.83	LPE (16:0)	7.80E + 06 ± 5.88E + 06 a	3.13E + 06 ± 1.18E + 06 a
92	38.35	LPE (18:1)	2.63E + 06 ± 1.25E + 06 a	2.58E + 06 ± 1.22E + 06 a
108	41.81	LPE (18:0)	3.42E + 08 ± 1.58E + 08 a	3.27E + 08 ± 6.09E + 07 a
		Fatty acid derivatives	3.26E + 08 ± 1.58E + 08 a	1.49E + 09 ± 1.11E + 09 a
28	28.69	9,12-Hexadecadienoic acid. 6-hydroxy-	9.49E + 06 ± 9.57E + 06 a	1.03E + 08 ± 1.15E + 08 a
32	29.58	9-Tetracosenoic acid*	1.98E + 07 ± 1.75E + 07 a	4.27E + 07 ± 5.87E + 07 a

Table 2 (continued)

Nº	RT[a] (min)	Possible annotation	Rainy	Dry
38	30.61	3,6-Pentadecadienedioic acid	1.04E + 07 ± 1.23E + 07 a	5.16E + 06 ± 1.13E + 06 a
41	30.80	15-Tetracosenoic acid	6.81E + 07 ± 6.82E + 07 a	6.92E + 06 ± 1.62E + 06 a
42	31.15	9,10,12-Trihydroxyoctadecanoic acid	3.09E + 06 ± 1.96E + 06 a	1.28E + 08 ± 1.24E + 08 a
43	**31.23**	**Oxooleic acid**	**2.22E + 06 ± 1.43E + 06 b**	**1.55E + 08 ± 1.25E + 08 a**
45	**31.73**	**4,9,11-Pentadecatrienoic acid. 15-hydroxy-**	**2.15E + 06 ± 1.88E + 06 b**	**3.20E + 08 ± 2.23E + 08 a**
46	**31.83**	**7-Hexadecenoic acid. 16-hydroxy-**	**4.26E + 06 ± 4.88E + 06 b**	**2.74E + 08 ± 2.17E + 08 a**
48	**32.46**	**4,9,11,13-Pentadecatetraenoic acid. 15-hydroxy-**	**2.65E + 06 ± 2.06E + 06 b**	**7.15E + 07 ± 5.71E + 07 a**
51	33.02	Oleic acid	1.01E + 08 ± 1.14E + 08 a	4.48E + 07 ± 3.60E + 07 a
54	**33.32**	**Eicosanolactone**	**4.99E + 07 ± 3.26E + 07 a**	**1.20E + 08 ± 4.81E + 07 b**
55	33.38	Pentacosanoic acid	4.04E + 06 ± 3.52E + 06 a	3.48E + 06 ± 1.90E + 06 a
59	34.23	2-Nonadecylbutanedioic acid	5.73E + 06 ± 3.51E + 06 a	4.66E + 07 ± 3.92E + 07 a
66	35.65	Pinolenic acid	6.36E + 06 ± 6.52E + 06 a	1.52E + 07 ± 8.96E + 06 a
82	37.27	9S-Hydroxy-10E,12Z,15Z-octadecatrienoic acid*	3.63E + 06 ± 2.41E + 06 a	8.79E + 07 ± 1.21E + 08 a
84	**37.41**	**19-Hydroxynonadecanoic acid**	**5.34E + 06 ± 3.88E + 06 b**	**3.69E + 07 ± 2.48E + 07 a**
91	**38.23**	**Linolenic acid***	**2.76E + 06 ± 1.41E + 06 b**	**9.48E + 07 ± 1.30E + 08 a**
95	39.20	13S-Hydroxy-9Z,11E,15Z-octadecatrienoic acid*	2.65E + 06 ± 6.32E + 05 a	5.01E + 07 ± 8.33E + 07 a
		Soluble sugar	1.63E + 07 ± 1.02E + 07 a	2.57E + 07 ± 7.99 E + 06 a
1	1.47	Melezitose	1.34E + 07 ± 1.06E + 07 a	2.03E + 07 ± 6.05E + 06 a
2	1.94	Galactopinitol A	2.89E + 06 ± 2.64E + 06 a	5.36E + 06 ± 2.55E + 06 a
		Terpenoid		
69	**35.97**	**Strobilactona A**	**1.97E + 07 ± 1.60E + 07 b**	**5.98E + 07 ± 2.82E + 07 a**
		Nucleotide	9.93E + 06 ± 9.87E + 06 a	2.02E + 07 ± 1.01E + 07 a
5	**2.04**	**3'-**Guanylic acid	**1.55E + 06 ± 1.08E + 06 b**	**4.94E + 06 ± 2.56E + 06 a**
6	2.08	Adenosine*	5.99E + 06 ± 6.36E + 06 a	1.23E + 07 ± 6.72E + 06 a
7	2.11	5'-Adenylic acid	9.66E + 05 ± 1.16E + 06 a	1.98E + 06 ± 8.31E + 05 a
10	3.67	N6-Threonylcarbamoyladenosine	1.42E + 06 ± 1.36E + 06 a	1.03E + 06 ± 2.86E + 05 a
		Phenolic	1.73E + 08 ± 9.69E + 07 a	2.14E + 08 ± 6.60E + 07 a
29	29.12	Tephrosin*	5.05E + 07 ± 4.28E + 07 a	2.21E + 07 ± 2.45E + 07 a
60	**34.28**	**Arachidin 3***	**3.46E + 06 ± 1.30E + 06 b**	**4.33E + 07 ± 6.28E + 07 a**
62	34.97	[7-(3,4-dihydroxyphenyl)-1-(4-hydroxyphenyl)heptan-3-yl] acetate	6.92E + 07 ± 4.51E + 07 a	4.26E + 07 ± 1.51E + 07 a
63	34.99	Cercosporin	6.75E + 06 ± 4.86E + 06 a	4.04E + 07 ± 5.33E + 07 a
77	36.72	3,3',4,5,5'-Pentamethoxystilbene*	2.87E + 07 ± 4.27E + 07 a	1.74E + 07 ± 1.94E + 07 a
83	37.38	Flavestin	2.29E + 06 ± 1.00E + 06 a	8.25E + 06 ± 7.81E + 06 a
112	**44.5**	**Dipetalolactone***	**1.19E + 07 ± 8.13E + 06 b**	**3.99E + 07 ± 3.27E + 07 a**
		Nitrogen compounds	3.99E + 08 ± 2.77E + 08 a	4.94E + 08 ± 1.67E + 08 a
19	21.75	3-Pyridinecarboxylic acid. 1,6-dihydro-5-methoxy-6-oxo-	5.55E + 06 ± 5.28E + 06 a	2.39E + 06 ± 2.03E + 06 a
53	33.22	Phytosphingosine	6.13E + 06 ± 3.97E + 06 a	4.87E + 06 ± 4.43E + 06 a
56	33.78	Cocamidopropylbetaine	7.49E + 07 ± 8.56E + 07 a	9.66E + 06 ± 6.08E + 06 a
85	37.48	Asperphenamate	5.28E + 07 ± 3.58E + 07 a	8.98E + 07 ± 7.56E + 07 a
111	42.87	Pheophorbide*	1.22E + 07 ± 1.31E + 07 a	9.16E + 07 ± 1.17E + 08 a
114	46.16	Docosenamide dimer	9.50E + 06 ± 1.42E + 07 a	2.77E + 06 ± 1.31E + 06 a
		Others		
94	39.05	Tris(2-butoxyethyl) phosphate	2.11E + 07 ± 3.97E + 06 a	2.22E + 07 ± 6.22E + 06 a

Different letters indicate significant differences between rainy and dry seasons ($P < 0.05$, $n = 5$) and are highlighted in bold

*Compounds with non-normal distribution

[a]*RT* retention time

and trisaccharides), amino acids, carboxylic acids, low mass phenolic compounds, ascorbate derivatives, and other nitrogen compounds (Supplementary Table S2). The major compounds in this phase were sucrose, followed by glucose and fructose.

Samples collected during the rainy season showed a higher abundance of monosaccharides, especially fructose and glucose, while samples collected during the dry season showed a high abundance of the disaccharide trehalose. In general, carboxylic acids showed no significant abundance variation between seasons, except for methylmalonic acid which was detected in higher abundance in the rainy season. Amino acids, such as gamma-aminobutyric acid (GABA) and asparagine, also showed significantly higher levels during the rainy season (Table 3).

The non-polar phase analyzed by GC–MS showed 63 compounds grouped in eight major classes: alkane, alkene, alcohol, fatty acids, terpenes (diterpenes and triterpenes), steroids, phenolic compounds, and other aromatic compounds (Supplementary Table S3). Fatty acids and steroids were the major classes detected in *C. purpureus*. Palmitic (C16:0), oleic (C18:1), and stearic (C18:0) were the major fatty acids observed, but significantly high abundances during the dry season were detected only for lignoceric (C24:0) and cerotic (C26:0) acids during the dry season. On the other hand, myristic (C14:0) and pentadecanoic (C15:0) acids, for example, showed higher abundances during the rainy season. Campesterol and stigmasterol were the major steroids detected, but significantly higher abundance was observed for β-sitosterol during the dry season (Table 4). Also in the non-polar phase, alpha-tocopherol and retinol could be found and were more abundant during the dry season.

Redox status

All enzymes analyzed (CAT, APX, SOD, and GR) are associated with the antioxidant cycle and they all showed significantly higher activity during the dry season. Also, during the dry season, ascorbate and glutathione showed significantly higher contents of their reduced forms, as well as, the ratios between the reduced form and total were significantly higher during the dry season. The four carotenoids found (lutein, β-carotene, violaxanthin, and neoxanthin) also showed significantly higher contents during the dry season.

Hydrogen peroxide (H_2O_2), hydroxyl radical ($^{\bullet}OH$), and superoxide radical (O_2^-) were detected in higher amounts in samples collected during the dry season. As well, higher content of MDA was detected during the dry season (Table 5).

Multivariate analysis

Twelve principal components were resumed by the PCA analysis and the first 5 components explained 58% of the data variability (Fig. 2). On the negative side of Axis 1 samples collected in the rainy season showed close chemical patterns between intracellular extract and cell wall conjugated compounds, forming one group (G1). This group is characterized by high amounts of prenylated and glycosylated flavonoids and fatty acids esters, suggesting that these compounds seem to be related to high temperatures, humidity, and total precipitation registered during the rainy season. Samples collected in the dry season clustered into two groups revealing different quantitative chemical patterns. The insoluble fraction was characterized mainly by the abundance of fatty acid derivatives and other flavonoids (G3), while the intracellular extracts (G2) correlated with high amounts of biflavonoids, other phenolics, and phospholipids (Fig. 2).

Discussion

Bryophytes are described as poikilohydric organisms, meaning that their water content varies according to environmental conditions, a condition lost in most tracheophyte species (Liu et al. 2019). Plants are often classified as drought-sensitive or drought-tolerant, but some species, as many bryophytes, can survive at relative water contents below 10% for long or short periods, being called desiccation-tolerant or resurrection plants (Porembski 2011).

Some mechanisms related to drought tolerance include growth inhibition during severe stress conditions, shedding of leaves, water use restriction of source tissues, and regulation of transpiration. These responses are essential to maintain the plant water status and carbon assimilation during dehydration conditions. Drought-tolerant plants can withstand prolonged water limitations by employing diverse physiological, biochemical, and molecular mechanisms such as succulence in leaves, deep roots, wax surfaces, or specialized photosynthetic pathways (Fernández-Marín et al. 2013; Liu et al. 2019). However, most of the studies involving desiccation-tolerant plants were done using angiosperm species, while bryophytes were used in very few studies.

It is important to point out the differences between these two groups of land plants. Besides the vascular/non-vascular difference between these groups, when studying bryophytes, the gametophyte is the dominant and perennial phase, while in angiosperms, the sporophyte is the phase accessed. According to Oliver et al. (2000), tolerance to vegetative desiccation among land plants is most certainly present in the basal groups, an important adaptive trait to primitive terrestrial forms during plant land colonization. For some

Table 3 Relative abundance of metabolites (μg g^{-1} DW) detected by GC–MS in the gametophyte' polar phase of *Ceratodon purpureus* from Campos do Jordão collected during the rainy and the dry seasons.

RT[a] (s)	Class	Probable compounds	Season	
			Rainy	Dry
	Monosaccharides		**1519.87 ± 1053.32 a**	**255.94 ± 171.72 b**
1544		Ribose	0.75 ± 0.64 a	0.19 ± 0.11 a
1806		**D-fructose**[b]	**681.76 ± 468.77 a**	**30.43 ± 21.36 b**
1827		D-mannose	4.01 ± 3.88 a	0.23 ± 0.43 a
1836		**D-glucose**[c]	**796.09 ± 546.00 a**	**34.84 ± 23.57 b**
1872		D-galactose	35.65 ± 42.23 a	190.13 ± 130.77 a
1919		Galacturonic acid	0.11 ± 0.11 a	0.12 ± 0.16 a
	Polyol		71.33 ± 54.54 a	48.01 ± 33.39 a
1812		Mannitol	0.55 ± 0.28 a	0.29 ± 0.23 a
1881		L-iditol	3.44 ± 5.12 a	8.22 ± 6.94 a
1989		*Scyllo*-inositol	0.24 ± 0.21 a	1.03 ± 1.11 a
2057		*Myo*-inositol	67.07 ± 50.50 a	38.47 ± 26.21 a
	Disaccharides		727.71 ± 566.85 a	2229.42 ± 1558.29 a
2589		Sucrose[d]	725.47 ± 567.70 a	2194.47 ± 1538.43 a
2651		α-Lactose	0.79 ± 0.80 a	0.68 ± 0.57 a
2679		**D-trehalose**[e]	**1.41 ± 0.87 b**	**34.25 ± 26.14 a**
2724		Maltose[f]	0.02 ± 0.02 a	0.02 ± 0.03 a
2936		Melibiose	0.03 ± 0.03 a	0.01 ± 0.01 a
	Amino acid		**126.27 ± 62.69 a**	**39.88 ± 27.41 b**
676		Sarcosine	2.78 ± 2.73 a	0.06 ± 0.08 a
802		L-norleucine	6.41 ± 7.69 a	0.16 ± 0.08 a
882		L-norvaline	0.11 ± 0.21 a	0.09 ± 0.14 a
982		L-proline	37.50 ± 57.56 a	24.16 ± 28.39 a
1107		L-alanine	25.35 ± 22.79 a	0.68 ± 0.69 a
1147		L-threonine	0.04 ± 0.06 a	0.05 ± 0.05 a
1212		L-aspartic acid	1.59 ± 1.97 a	0.77 ± 0.98 a
1353		L-5-oxoproline	33.35 ± 31.20 a	10.62 ± 15.65 a
1360		**GABA**	**4.62 ± 3.12 a**	**0.25 ± 0.46 b**
1372		L-glutamic acid	0.01 ± 0.02 a	0.07 ± 0.07 a
1419		L-serine	0.70 ± 0.65 a	0.07 ± 0.07 a
1565		**L-asparagine**	**9.05 ± 6.04 a**	**0.44 ± 0.23 b**
	Carboxylic acid		194.64 ± 161.79 a	147.88 ± 188.51 a
716		Oxalic acid	6.45 ± 8.44 a	0.00 ± 0.00 a
766		Hydroxybutyric acid	15.88 ± 9.92 a	9.31 ± 10.71 a
784		Malonic acid	13.36 ± 4.29 a	17.51 ± 8.93 a
851		3-Methyl-2-oxovaleric acid	0.33 ± 0.49 a	0.03 ± 0.03 a
874		**Methylmalonic acid**	**10.80 ± 5.49 a**	**1.34 ± 2.68 b**
1019		Nicotinic acid	2.24 ± 2.43 a	0.50 ± 0.57 a
1042		Succinic acid	1.70 ± 3.31 a	0.88 ± 1.75 a
1101		Fumaric acid	17.27 ± 15.01 a	0.32 ± 0.34 a
1254		Phenylpropionic acid	0.56 ± 0.43 a	0.15 ± 0.12 a
1303		Malic acid	118.18 ± 130.40 a	64.45 ± 70.62 a
1663		Aconitic acid	0.01 ± 0.01 a	0.02 ± 0.02 a
1747		Citric acid	10.03 ± 9.16 a	4.29 ± 6.82 a
1842		Ascorbic acid	1.71 ± 1.45 a	0.52 ± 0.32 a
	Nitrogen		9.91 ± 10.12 a	1.02 ± 1.11 a
679		Hydroxylamine	1.10 ± 1.02 a	0.47 ± 0.58 a
955		**3-aminopropionitrile**	**6.24 ± 8.00 a**	**0.01 ± 0.02 b**
1019		Nicotinic acid	2.24 ± 2.43 a	0.50 ± 0.57 a

Table 3 (continued)

RT[a] (s)	Class	Probable compounds	Season	
			Rainy	Dry
1117		2,3-Diaminopropionic acid	0.24 ± 0.14 a	0.08 ± 0.13 a
	Phenolic		**14.28 ± 1.42 a**	**5.37 ± 3.98 b**
942		**Benzoic acid**	**5.04 ± 0.22 a**	**1.55 ± 1.96 b**
1125		***o*-toluic acid**	**9.20 ± 1.30 a**	**3.82 ± 2.68 b**
	Others			
758		Dihydrouracil	0.33 ± 0.63 a	0.04 ± 0.03 a
1791		Shikimic acid	0.04 ± 0.05 a	0.00 ± 0.00 a
2488		Uridine	0.24 ± 0.14 a	1.35 ± 1.40 a

Different letters indicate significant differences between rainy and dry seasons ($P < 0.05$, $n = 5$) and are highlighted in bold

[a]*RT* retention time

[b]Fructose stereoisomers

[c]Glucose stereoisomers

[d]Sucrose stereoisomers

[e]D-Trehalose stereoisomers

[f]Maltose stereoisomers

authors, desiccation tolerance was lost during land plant evolution, maintained only in reproductive tissues, which can be corroborated by the production of desiccation-tolerant structures such as seeds and pollen in spermatophytes (Oliver et al. 2000). Thus, seed and pollen desiccation-tolerant mechanisms might be more similar to the ones shown by bryophyte gametophytes than to the desiccant-tolerant angiosperm sporophytes.

C. purpureus in its natural environment is continuously subjected to desiccation–rehydration cycles throughout seasons, showing gametophyte' lipid and sugar metabolism alterations similar to those reported for angiosperms drought-tolerant species.

Two large classes of lipids found in *C. purpureus* were LPC and LPE, the most abundant phospholipids in extra plastid membranes (Nerlich et al. 2007). Those classes are generally involved in plant defense systems, increasing their abundance during exposure to pathogens and wounding by herbivores (Lee et al. 1997; Chen et al. 2019). Previous reports proposed that these phospholipids in *C. purpureus* are involved in the defense system, mainly enhancing the cell's ability to acquire frost hardiness, allowing rapid cell membrane repair after frost stress, remembering that this species is found in Antarctica (Aro and Karunen 1988). Frost stress triggers some similar responses as drought; both stresses alter lipid and sugar metabolisms to provide not only osmoprotection but also protect membranes through the interaction with the lipid bilayer (Sami et al. 2016). High content of these phospholipids was observed in *C. purpureus* during the dry season, corroborating their involvement in the plant defense system against harsher environmental conditions, in this case, low temperature and low rainfall.

Lipid metabolism differed between seasons in *C. purpureus* also regarding fatty acid abundance and its derived classes (alcohols, alkanes, and alkenes). Palmitic (C16:0), oleic (C18:1), and stearic (C18:0) were the major fatty acids detected for this species, but significant abundance variation between seasons was observed for lignoceric (C24:0) and cerotic (C26:0) acids, which accumulated during the dry season. Under desiccation, the content of neutral lipids usually increases and the degree of unsaturation is reduced (Goss and Wilhelm 2009), which corroborates the high accumulation of longer saturated fatty acids during the dry season in *C. purpureus*.

Long-chain fatty acids found in *C. pupureus* are among the common ones in occurrence in bryophytes. Bryophytes and algae commonly produce high amounts of long-chain and very-long-chain fatty acids (above C20), and also their polyunsaturated version, such as arachidonic acid (C20:4), but these fatty acids are rarely found in spermatophytes (Goss and Wilhelm 2009; Klavina 2018; Lu et al. 2019). This fatty acid composition suggests that evolution to the latter groups of land plants prioritized shorter chains and less saturated fatty acids at the expense of long chains and highly unsaturated ones (Goss and Wilhelm 2009; Lu et al. 2019). Regarding the seasonality role on fatty acid metabolism, in *Sphagnum palustre* L., high amounts of long-chain fatty acids were detected under dryer conditions, but when the water supply was available, this species showed high amounts of shorter chain fatty acids (Huang et al. 2012). *C. purpureus* showed high abundances of longer saturated lignoceric (C24:0) and cerotic (C26:0) acids in the dry season, corroborating previous studies.

Table 4 Relative abundance of metabolites (μg g^{-1} DW) detected by GC–MS in the gametophyte' non-polar phase of *Ceratodon purpureus* from Campos do Jordão collected during the rainy and the dry seasons.

RT[a] (s)	Class	Probable compounds	Season	
			Rainy	Dry
	Alcohol		**66.47 ± 13.00 a**	**19.75 ± 5.40 b**
1159		**Tetradecanol**	**40.48 ± 7.55 a**	**12.42 ± 2.70 b**
1246		Pentadecanol	1.16 ± 0.98 a	0.51 ± 0.30 a
1414		**Hexadecanol**	**11.79 ± 2.19 a**	**2.84 ± 1.07 b**
1646		**Octadecanol**	**3.61 ± 0.40 a**	**1.03 ± 0.50 b**
1687		**Nonadecanol**	**8.73 ± 1.64 a**	**2.02 ± 0.52 b**
1989		Docosanol	0.70 ± 0.35 a	0.93 ± 0.27 a
	Alkane		**17.90 ± 2.19 a**	**5.72 ± 2.19 b**
928		Hexadecane	0.11 ± 0.06 a	0.08 ± 0.03 a
1062		**Heptadecane**	**0.04 ± 0.01 b**	**1.39 ± 1.16 a**
1216		**Octadecane**	**1.45 ± 0.30 a**	**0.39 ± 0.10 b**
1356		**Nonadecane**	**10.99 ± 1.67 a**	**2.84 ± 0.81 b**
1407		**Eicosane**	**1.76 ± 0.38 a**	**0.16 ± 0.18 b**
1554		**Heneicosane**	**3.31 ± 0.70 a**	**0.80 ± 0.31 b**
1969		**Pentacosane**	**0.24 ± 0.15 a**	**0.06 ± 0.02 b**
	Alkene		**21.57 ± 5.06 a**	**4.48 ± 2.38 b**
1167		**Octadecene**	**0.49 ± 0.15 a**	**0.12 ± 0.05 b**
1318		**Nonadecene**	**5.53 ± 0.89 a**	**1.47 ± 0.63 b**
1432		**Eicosene**	**12.14 ± 2.28 a**	**2.21 ± 1.13 b**
2106		**Heptacosene**	**3.28 ± 1.21 a**	**0.66 ± 0.43 b**
2273		**Octacosene**	**0.13 ± 0.09 a**	**0.03 ± 0.02 b**
	Fatty acids		**986.74 ± 270.53 a**	**530.31 ± 161.78 b**
723		**Decanoic acid**	**0.45 ± 0.07 a**	**0.21 ± 0.08 b**
1004		**Dodecanoic acid**	**1.17 ± 0.18 a**	**0.43 ± 0.27 b**
1198		Azelaic acid	1.09 ± 0.16 a	0.92 ± 0.29 a
1255		**Myristic acid**	**15.54 ± 3.40 a**	**4.41 ± 1.98 b**
1372		**Pentadecanoic acid**	**9.15 ± 2.17 a**	**2.07 ± 1.50 b**
1453		**Palmitoleic acid**	**0.65 ± 0.47 a**	**0.07 ± 0.13 b**
1483		**Palmitic acid**	**501.91 ± 101.20 a**	**220.50 ± 43.00 b**
1664		Oleic acid	103.89 ± 63.36 a	119.24 ± 97.11 a
1672		Elaidic acid	7.33 ± 3.14 a	4.81 ± 4.47 a
1693		**Stearic acid**	**303.45 ± 53.98 a**	**120.32 ± 39.09 b**
1753		Linoleic acid	3.66 ± 2.99 a	2.17 ± 0.75 a
1812		Arachidonic acid	14.49 ± 12.99 a	3.28 ± 1.00 a
2214		Nervonic acid	0.49 ± 0.65 a	0.76 ± 0.55 a
2235		**Lignoceric acid**	**9.33 ± 4.74 b**	**20.82 ± 7.71 a**
2392		**Hexacosanoic acid**	**6.41 ± 3.56 b**	**23.30 ± 3.48 a**
2541		Octacosanoic acid	5.17 ± 6.26 a	5.13 ± 1.23 a
	Steroid		164.55 ± 101.83 a	181.23 ± 32.48 a
2551		Epicampesterol	65.63 ± 31.08 a	85.21 ± 13.91 a
2559		**β-sitosterol**	**0.73 ± 0.39 b**	**4.77 ± 0.95 a**
2615		Stigmasterol	98.19 ± 60.60 a	91.25 ± 15.55 a
	Triterpenoid		4.28 ± 3.73 a	2.76 ± 1.05 a
2220		Squalene	5.85 ± 4.21 a	2.71 ± 1.09 a
2656		Lanosterol	1.64 ± 2.03 a	0.08 ± 0.07 a
	Ester		99.84 ± 60.55 a	25.36 ± 10.04 a
1237		11-Tetradecen-1-ol, acetate	17.49 ± 14.29 a	6.86 ± 2.55 a
1657		Linoleic acid ethyl ester	75.15 ± 49.15 a	17.56 ± 9.77 a
2035		**1-monopalmitin**	**7.21 ± 5.03 a**	**0.95 ± 0.22 b**

Table 4 (continued)

RT[a] (s)	Class	Probable compounds	Season	
			Rainy	Dry
	Diterpenoid		6.32 ± 5.05 a	4.12 ± 1.43 a
1569		Isophytol	0.01 ± 0.02 a	0.02 ± 0.01 a
1626		Phytol	13.16 ± 9.41 a	4.67 ± 1.47 a
1731		Pimaric acid	0.00 ± 0.00 a	0.01 ± 0.01 a
	Vitamins		**11.72 ± 5.86 b**	**21.53 ± 4.39 a**
1913		**Retinol**	**0.00 ± 0.00 b**	**0.03 ± 0.03 a**
2473		**Alpha-tocopherol**	**11.72 ± 5.86 b**	**21.50 ± 4.57 a**
	Nucleoside		**14.05 ± 3.68 a**	**4.69 ± 3.59 b**
2358		**Guanosine**	**14.05 ± 3.29 a**	**4.70 ± 3.28 b**
	Others			
570		*o*-Toluic acid	0.67 ± 0.63 a	1.03 ± 0.40 a
768		**3,4-Dimethylbenzoic acid**	**0.39 ± 0.10 a**	**0.14 ± 0.03 b**
816		**2,4-Di-tert-butylphenol**	**1.87 ± 0.22 a**	**0.00 ± 0.00 b**
1186		Glycerol 1-phosphate	5.39 ± 5.11 a	5.44 ± 3.05 a
1827		16-Hydroxyhexadecanoic acid	2.56 ± 1.87 a	1.86 ± 1.31 a
1848		**Nonyl tetracosyl ether**	**5.61 ± 1.50 a**	**0.86 ± 0.49 b**
1908		**Myo-inositol 1-phosphate**	**0.50 ± 0.37 b**	**2.87 ± 1.92 a**
2082		**Octadecyl octyl ether**	**5.90 ± 1.50 a**	**1.04 ± 0.66 b**
2129		Alpha lactose	0.31 ± 0.29 a	5.05 ± 10.54 a
2136		Maltose	0.01 ± 0.01 a	0.35 ± 0.77 a
2243		Maltitol	0.40 ± 0.14 a	0.14 ± 0.11 a
2443		**Docosyl octyl ether**	**0.21 ± 0.10 a**	**0.05 ± 0.02 b**
2641		12-Oleanen-3-yl acetate	0.59 ± 0.78 a	0.14 ± 0.06 a
2697		Alpha-spinasterol acetate	0.85 ± 0.97 a	0.21 ± 0.06 a

Different letters indicate significant differences between rainy and dry seasons ($P < 0.05$, $n = 5$) and are highlighted in bold

[a]*RT* retention time

C. purpureus also showed differences in sugar metabolism between seasons. Sucrose followed by glucose and fructose were the major sugars found in this species, which corroborates sucrose being commonly described as the most abundant soluble sugar in bryophytes (Green et al. 2011; Pejin et al. 2012).

Drought tolerance relies on the ability to keep cellular integrity during desiccation and on the repair of induced cellular damage upon rehydration. Strategies used by desiccation-tolerant plants include the shut-down of photosynthesis, ROS scavenging systems, the accumulation of sugars, and the enrichment of transcripts associated with cell wall plasticity also detected in seeds (Williams et al. 2015). In seeds was observed the importance of cell viscosity during desiccation, which increases with the decrease of cell water content, leading to a highly viscous liquid cytoplasm, allowing molecular diffusion but decreasing chemical reactions (Fernández-Marín et al. 2013). As mentioned before, freezing also leads to desiccation that accompanies extracellular ice formation. In both situations, adjusting the cell's solute concentrations seem to be one of the strategies to survive to significant temperature and water fluctuations (Lenné et al. 2010; Fernández-Marín et al. 2013).

The high contents of disaccharides, such as sucrose and trehalose were also described for the moss *Physcomitrella patens*. Under cold stress, *P. patens* showed an increase in sugar contents, especially the levels of trehalose, isomaltose, and maltose (Arif et al. 2018), as well as these disaccharides increased against the effects of low air humidity and high temperature (Oldenhof et al. 2006). The increased sugar contents in *P. patens* were explained by the degradation of starch also observed under drought stress (Erxleben et al. 2012). *C. purpureus* under freezing conditions showed cell desiccation induced by external ice together with increased levels of sucrose and trehalose (Lenné et al. 2010). Although, according to the authors, the sugar concentrations alone were not sufficient to confer freezing tolerance, but were important osmoprotectants associated with the cavitation and embolism of hydroid cells and the decrease to ~ 20% of the original volume of the parenchyma cells (Lenné et al. 2010).

Trehalose is associated with protection during stressful periods by stabilizing biostructures, such as proteins and

Table 5 Redox status in *Ceratodon purpureus* collected in the rainy and the dry seasons

Compounds	Season	
	Rainy	Dry
Enzymatic		
CAT	2.33 ± 1.68 b	11.88 ± 7.07 a
APX	0.17 ± 0.09 b	0.42 ± 0.25 a
GR	0.12 ± 0.08 b	0.25 ± 0.16 a
SOD	0.43 ± 0.30 b	2.14 ± 1.08 a
Non-enzymatic		
AsA	1.36 ± 0.04 b	13.27 ± 1.47 a
DHA	2.45 ± 1.23 b	16.92 ± 6.43 a
AsA + DHA	3.77 ± 1.39 b	30.20 ± 10.83 a
Ratio (AsA/AsA + DHA)	0.37 ± 0.09 b	0.57 ± 0.15 a
GSH	1.15 ± 0.57 b	22.07 ± 3.08 a
GSSG	1.52 ± 1.21 a	1.80 ± 1.57 a
GSH + GSSG	2.67 ± 1.79 b	24.31 ± 3.11 a
Ratio (GSH/GSH + GSSG)	0.46 ± 0.10 b	0.94 ± 0.06 a
Reactive oxygen species		
H_2O_2	0.02 ± 0.01 b	0.05 ± 0.01 a
$^{\bullet}OH$	14.66 ± 4.21 b	58.06 ± 3.07 a
$O_2^{\bullet-}$	27.76 ± 8.58 b	100.89 ± 14.01 a
Indicator of lipid peroxidation		
MDA	0.02 ± 0.01 b	0.16 ± 0.03 a
Carotenoids		
Lutein	2.73 ± 1.33 b	15.83 ± 2.78 a
β-carotene	7.00 ± 2.31 b	44.09 ± 8.36 a
Neoxanthin	0.42 ± 0.33 b	2.55 ± 0.50 a
Violaxanthin	0.41 ± 0.11 b	1.33 ± 0.23 a

Mean values ± standard deviation ($n = 5$) of enzymatic activity: catalase CAT µmol min^{-1} mg^{-1} protein DW ascorbate peroxidase APX µmol min^{-1} mg^{-1} protein DW, glutathione reductase *GR* µmol min^{-1} mg^{-1} protein DW, and superoxide dismutase *SOD* U min^{-1} mg^{-1} protein DW, non-enzymatic compounds: ascorbic acid (µg g^{-1} DW) in its reduced (AsA), oxidized (DHA) and total (AsA + DHA) forms, and AsA/AsA + DHA ratio, glutathione (µg g^{-1} DW) in its reduced (GSH), oxidized (GSSG), and total (GSH + GSSG) forms, and GSH/GSH + GSSG ratio; reactive oxygen species: hydrogen peroxide (H_2O_2 µmol g^{-1} DW), hydroxyl radical (•OH % of 2′-deoxyribose oxidative degradation DW), and superoxide (O_2^{-}; nmol g^{-1} DW); lipid peroxidation: malondialdehyde acid (MDA; mM DW); carotenoids (µg g^{-1} DW): lutein, β-carotene, neoxanthin, and violaxanthin. Different letters indicate significant differences between seasons measured by Holm-Sidak test ($P < 0.05$)

lipid membranes (Pereira et al. 2004; Bolouri-Moghaddam et al. 2010). *Tripogon loliiformis* showed the absence of cell death in dehydrated and desiccated tissues which was associated with accumulation of trehalose during dehydration and increased cell autophagy in dehydrating shoots (Williams et al. 2015). According to the authors, resurrection plants accumulate trehalose at levels that are too low to serve as either osmoprotectants or energy sources, but these levels trigger cell autophagy which may enable to retain cell viability even under extreme stress.

The low levels of reducing sugars, mainly glucose and fructose, in samples of *C. purpureus* from the dry season, may also prevent protein damage by non-enzymatic glycosylation, therefore some mosses often decrease their reducing sugar contents during desiccation (Smirnoff 1992). Another possibility of explaining the low levels of glucose is the fact that this compound is used as a precursor of glycolysis that enhances NADH or NADPH and the oxidative pentose phosphate pathway (OPP), thus enhancing the cellular defenses against hydrogen peroxide (Couée et al. 2006). Glucose is also the main carbon precursor for the synthesis of carotenoids, ascorbate, and the amino acids used in the production of glutathione (Couée et al. 2006), which were molecules that had increased abundances in *C. purpureus* during the dry period, contrasting with the decrease in glucose levels. Also, glucose and sucrose can act as a regulator of gene expression of several pathways involved in ROS protection, like the ascorbate biosynthesis, OPP pathway, carotenoid biosynthesis, and chalcone synthase activity, this last one an enzyme involved in the flavonoid biosynthesis (Couée et al. 2006).

During desiccation, photosynthesis-related genes are down-regulated and the xanthophyll cycle is among plant photoprotective mechanisms. The xanthophyll cycle consists of the enzymatic de-epoxidation of violaxanthin to antheraxanthin and zeaxanthin during periods of high light illumination, but the inverse during low light or darkness, restoring the epoxidized xanthophylls (Fernández-Marín et al. 2013). Nowadays, the main known xanthophyll cycles are the violaxanthin, reported for spermatophytes, green and brown algae, and the diadinoxanthin cycle in diatoms, haptophytes, and dinophytes. In addition, it was already reported the existence of a lutein epoxide cycle but restricted to some families of spermatophytes (Goss and Latowski 2020). These cycles act as an important protection mechanism against damage of the photosynthetic apparatus by supersaturating light conditions, as fluctuations of the light intensity induced by clouds or by rapid changes of the leaf coverage. Furthermore, xanthophyll cycles play an important role in the protection against oxidative stress generated not only by the excess of light but also by other factors like drought, chilling, heat, and senescence (Latowski et al. 2011).

C. purpureus showed higher levels of ROS during the dryer season, which seems to be quenching, in part, by the enzymatic and non-enzymatic antioxidant systems, since some damage to membranes was detected as higher levels of MDA. The higher concentration of ROS and MDA might explain the lower amounts of lipids during the dry season, probably due to higher lipid peroxidation. Also, the higher abundance of trehalose and the lower content of fructose and glucose during the dry season might represent the role

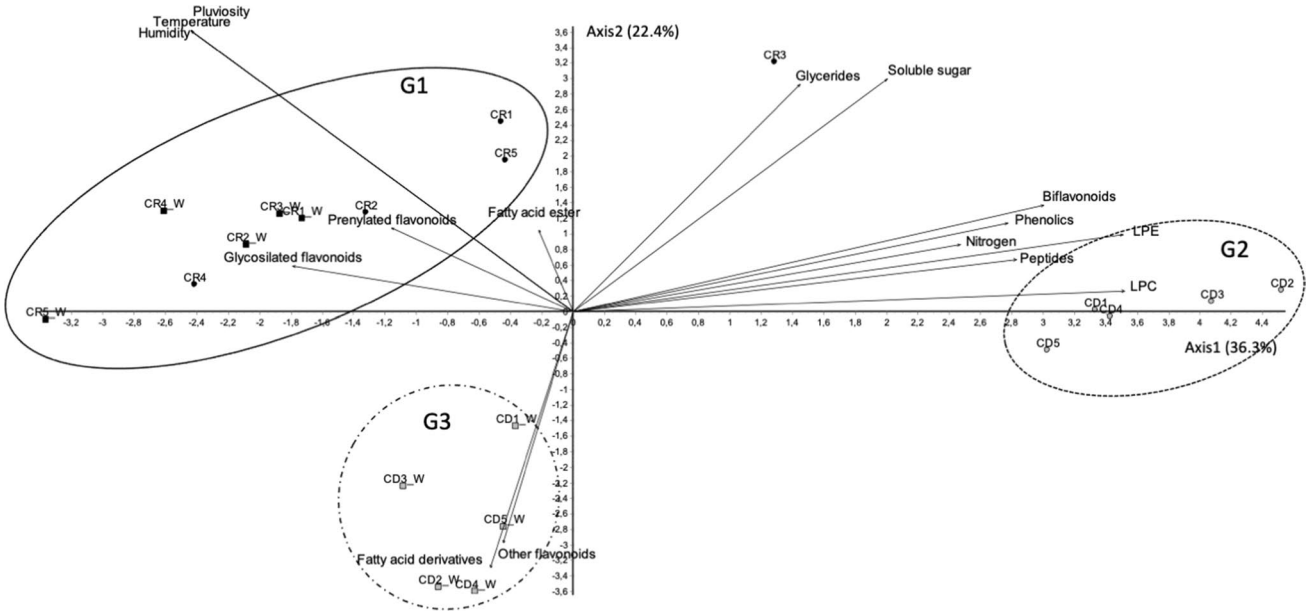

Fig. 2 Principal component analysis of major metabolites classes detected in *Ceratodon purpureus* collected in Campos do Jordão (São Paulo/Brazil). *G1* samples collected in the rainy season (intracellular and cell wall conjugated compounds); *G2* samples collected in the dry season (intracellular compounds); *G3* samples collected in the dry season (cell wall conjugated compounds); *CR* intracellular extracts from the rainy season; *CD*: intracellular extracts from the dry season; CR_W cell wall conjugated extracts from the rainy season; CD_W cell wall conjugated extracts from the dry season

of these sugars as antioxidants against increased ROS formation (Pereira et al. 2004; Bolouri-Moghaddam et al. 2010). Furthermore, phytosterols also have important roles during plant desiccation, as β-sitosterol which acts in two ways, reducing the generation of H_2O_2 and up-regulating the activity of antioxidant enzymes (SOD, CAT, POD, and APX), ascorbate, and carotenoid synthesis (Elkeilsh et al. 2019). In the dry season, *C. purpureus* showed high ROS production, a significantly higher concentration of β-sitosterol, together with increased amounts of ascorbate and carotenoids (including xanthophylls), as well as increased activity of the enzymatic antioxidant system.

The redox potential, characterized by the ratio between the reduced form and total ascorbate and glutathione in *C. purpureus* during the dry period suggests greater defense capacity of this species. The predominance of reduced forms of both AsA and GSH in plants under oxidative stress activates APX, which uses reduced ascorbate as a substrate to decompose H_2O_2 into H_2O, as well as GSH is used as a co-substrate to reduce H_2O_2 (Burkey et al. 2006). This can be related to the higher APX activity in samples collected in the dry season, where AsA and GSH contents were also higher.

The present study also provided important information regarding the polyphenol composition of *C. purpureus*. Waterman et al. (2017) studied populations of *C. purpureus* in Antarctica and Australia, reporting two biflavonoids varying in relative abundances and cellular location between populations. For the Antarctic samples, biflavonoids were 13-fold more abundant in crude cell wall extract than in the intracellular extract but were absent in the cell wall extracts obtained from the Australian samples. Five biflavonoids were reported by Waterman et al. (2017), being 5',8″-biluteolin and 2,3-dihydro-5′,3‴-dihydroxyamentoflavone the most abundant found both intracellular and bounded to Antarctic moss cell walls. Here, we annotated 8 biflavonoids, including 5′,8″-biluteolin [26], but only eriodictyol-(5'→8″)-quercetin [34] and luteolin-(5'→8″)-apigenin [44] showed significantly higher abundances in the dry season; the first one was found intracellular while the second one in the cell wall extract. *C. purpureus* is a cosmopolitan moss found in extremely cold environments to hot deserts, and its population from high-altitude rainforest in Brazil seems to exhibit a similar chemical pattern to the Australian population, showing biflavonoids mainly found in the intracellular extract. For Waterman et al. (2017), the location of biflavonoids and other phenolic compounds within the cell wall of the Antarctic population suggests their role in photoprotection against UV radiation, increased over the past four decades in the area. According to these authors, this variation might be related to environmental differences, different stress factors, and seasonality, corroborating our findings of a high abundance of biflavonoids during the dry season.

In opposition to the biflavonoids, which tend to be more abundant in intracellular extract during the dry season, prenylated flavonoids seem to be mostly found conjugated to the cell wall, especially in the rainy season, as [39], [49],

and [90]. Glycosylated flavonoids are also more abundant during the rainy season. Consequently, these data evince the possible participation of prenylated and glycosylated flavonoid groups in the acclimation of *C. purpureus* to the environmental conditions throughout seasons.

However, some specific flavonoids evade those group patterns. Luteolin 7-glucuronide [31], as well as the prenylated flavonoids [50], [61], and [75], showed higher intracellular abundance during the dry season than the rainy counterpart. Yet, a high amount of the formononetin derivative [113] was observed during the dry season, in the cell wall extract. Despite having no reports of prenylated flavonoids in bryophytes up to date, there are reports of other prenylated phenolic compounds, especially in liverworts, such as prenylated bybenzyls in the genera Radula and Thysananthus (Asakawa et al. 2013; Asakawa and Ludwiczuk 2018). There are also reports of prenylated phenanthrenequinone in the moss *Paraleucobryum longifolium (*Hedw.) Loeske (Csupor et al. 2020). For this class of flavonoids, annotation using data reported for *C. purpureus* or commercial standards was not possible, therefore, the GNPS suggestions on prenylated flavonoids must be taken by caution.

Most of the compounds showing significantly different relative abundances between seasons were plotted according to their biosynthesis pathways in Fig. 3. Lipid and sugar metabolism seemed to reduce during the dry season, except for phospholipids and long-chain fatty acids. On the other side, terpene synthesis (especially carotenoids) vitamins, and phenolic metabolism (particularly flavonoids) are enhanced during the dry season.

These changes show the metabolome fluctuations regarding seasonality and may indicate that *C. purpureus* is under harsher environmental conditions during the dry period, mainly due to low temperatures, high global solar radiation, and less water availability (low rainfall), although the average air humidity was not highly different between the dry and the rainy seasons. The Campos do Jordão population of this species can be found in open areas in the borders of the forest. During the rainy season, this moss can be found as green cushions growing directed on the soil (Fig. 4), but during the dry season, the desiccated cushions became brown and less distinctively in the environment. Furthermore, during the dry season daily maxima/minima temperatures registered in Campos do Jordão were 24.2 and − 0.6 °C, respectively, which also might contribute to these metabolome adjustments.

Conclusion

The metabolome approach pointed out changes in lipid, sugar, phenolic, and terpene metabolism of *Ceratodon purpureus* throughout annual seasons (rainy and dry seasons), and the cellular distribution of some constituents (intracellular and/or cell wall conjugated). Fatty acids and monosaccharides were more abundant during the rainy season, while some flavonoids and carotenoids (including xanthophylls) were more abundant during the dry season. Beyond that, biflavonoids tend to be mostly found intracellularly while prenylated flavonoids tend to be more present conjugated to the cell wall. These changes indicate

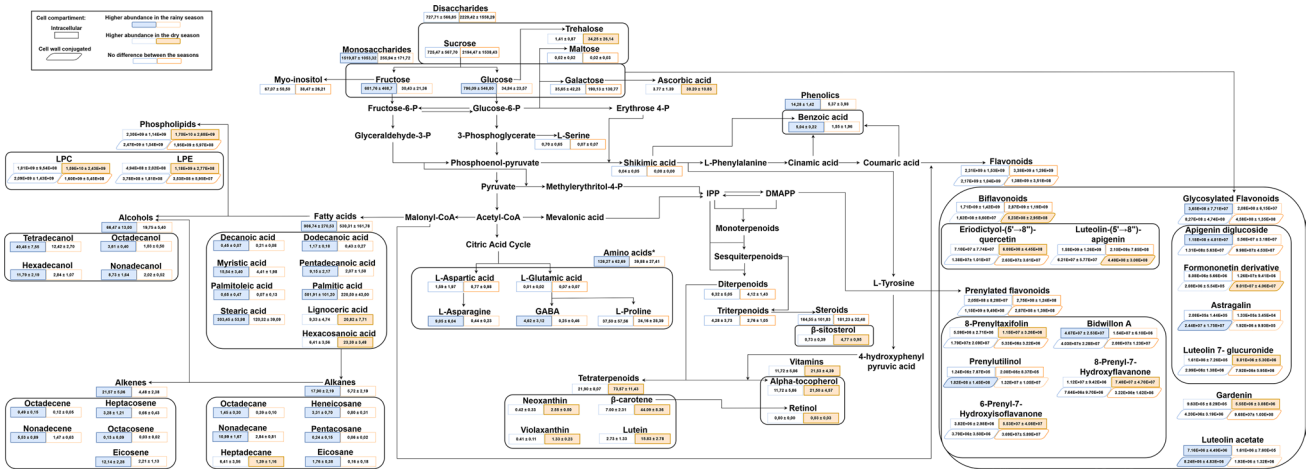

Fig. 3 Schematic biosynthetic pathways for metabolites annotated for *Ceratodon purpureus*. Blue and orange boxes indicate the relative abundance of a metabolite (or their chemical class group) detected in the rainy and in the dry seasons, respectively. Filled boxes show significantly higher abundances ($P < 0.05$, $n = 5$) comparing seasons. Ellipse and parallelogram boxes indicate the abundances of compounds in intracellular extracts and conjugated to cell walls, respectively. (*) represents metabolites also synthetized by other pathways different than the ones here illustrated. *DMAPP* dimethylallyl diphosphate, *GABA* γ-aminobutyrate, *IPP* isopentenyl diphosphate, *LPC* lysophosphatidylcholine, *LPE* lysophosphatidylethanolamine

Fig. 4 Place of plant collection in Campos do Jordão: **a** Landscape view. **b** *Ceratodon purpureus* green cushions growing directed in the soil

harsher environmental conditions in Campos do Jordão during the dry period, mainly due to low temperatures and scarce rainfall, directing metabolic precursors to enhance the antioxidant system, such as flavonoids, carotenoids, and disaccharides contents, as well as, high antioxidant enzyme activity.

C. purpureus population in its natural Brazilian habitat showed a chemical similarity pattern to the Australian population studied by Waterman et al. (2017), showing biflavonoids majorly found in the intracellular extracts and higher abundances during the dry season. Although the redox potential suggests greater defense capacity of this species during the dry period (high ratio between the reduced and total forms of ascorbate and glutathione, besides enhanced contents of antioxidant metabolites), it seems not to be efficient enough for ROS quenching, resulting in some level of lipid peroxidation showed by enhanced contents of MDA.

Author contribution statement RC, DFP, and CMF collected the plant material; CMF and RC designed the study; WRSC, FPMA, MPE prepared the extracts and conducted the chemical analyses; WRSC and FPMA conducted the HPLC–MS^{-2} and GC–MS analysis through GNPS platform and prepared the tables and the figures; MPE performed the enzyme analyses; MR collaborated with the analysis of carotenoids; WRSC, MPE, and CMF wrote the manuscript; FPMA, MPE, RC, DFP, and MR revised the manuscript. All authors approved the final version of the manuscript.

Supplementary Information The online version contains supplementary material available at https://doi.org/10.1007/s00425-022-03857-8.

Acknowledgements This work has been supported by Fundação de Amparo à Pesquisa do Estado de São Paulo (FAPESP; 2018/02751-7) and Coordenação de Aperfeiçoamento de Pessoal de Nível Superior–Brasil (CAPES; Finance Code 001). CMF, MR, and DFP are thankful to Conselho Nacional de Desenvolvimento Científico e Tecnológico (CNPq) for the research grants. MPE thanks Fundação de Amparo à Pesquisa do Estado de São Paulo (FAPESP; 2018/21011-4). Authors also thank the ChemAxon team for providing the academic license on Marvin Sketch, version 21.12, used to generate the chemical illustrations on Fig. 1.

Data availability The datasets generated during and/or analyzed during the current study are available in the GNPS repository: Deconvolution data from Non-polar phase: http://gnps.ucsd.edu/ProteoSAFe/status.jsp?task=63682beec58a42668b19dae88f6af49e Library search data from Non-polar phase: http://gnps.ucsd.edu/ProteoSAFe/status.jsp?task=9d4f9f35865047798b3d07becc108d38 Deconvolution data from the polar phase: http://gnps.ucsd.edu/ProteoSAFe/status.jsp?task=992d6321bbf24bb1a393b20a8accf680 Library search data from the polar phase: http://gnps.ucsd.edu/ProteoSAFe/status.jsp?task=67b349cdb795447e866d167ac550dabd FBMN from Soluble (Cytoplasm) and Insoluble (Cell-wall) extract: http://gnps.ucsd.edu/ProteoSAFe/status.jsp?task=7f4106151fea4b42bd48834e8901c6b1

Declarations

Conflict of interest The authors declare no conflicts of interest.

References

Alves FRR, Lira BS, Pikart FC et al (2020) Beyond the limits of photoperception: Constitutively active PHYTOCHROME B2 overexpression as a means of improving fruit nutritional quality in tomato. Plant Biotechnol J. https://doi.org/10.1111/pbi.13362

Arif MA, Alseekh S, Harb J et al (2018) Abscisic acid, cold and salt stimulate conserved metabolic regulation in the moss

Physcomitrella patens. Plant Biol 20:1014–1022. https://doi.org/10.1111/plb.12871

Aro E-M, Karunen P (1988) Effects of hardening and freezing stress on membrane lipids and CO_2 fixation of *Ceratodon purpureus* protonemata. Physiol Plant 74:45–52. https://doi.org/10.1111/j.1399-3054.1988.tb04939.x

Asakawa Y, Ludwiczuk A, Nagashima F (2013) Phytochemical and biological studies of bryophytes. Phytochemistry 91:52–80. https://doi.org/10.1016/j.phytochem.2012.04.012

Asakawa Y, Ludwiczuk A (2018) Chemical constituents of bryophytes: structures and biological activity. J Nat Prod 81:641–660. https://doi.org/10.1021/acs.jnatprod.6b01046

Biersma EM, Convey P, Wyber R et al (2020) Latitudinal biogeographic structuring in the globally distributed moss *Ceratodon purpureus*. Front Plant Sci 11:502359. https://doi.org/10.3389/fpls.2020.502359

Bolouri-Moghaddam MR, Le Roy K, Xiang L et al (2010) Sugar signalling and antioxidant network connections in plant cells. FEBS J 277:2022–2037. https://doi.org/10.1111/j.1742-4658.2010.07633.x

Bowman JL, Kohchi T, Yamato KT et al (2017) Insights into land plant evolution garnered from the *Marchantia polymorpha* genome. Cell 171:287-304.e15. https://doi.org/10.1016/j.cell.2017.09.030

Burkey KO, Neufeld HS, Souza L et al (2006) Seasonal profiles of leaf ascorbic acid content and redox state in ozone-sensitive wildflowers. Env Pollut 143:427–434. https://doi.org/10.1016/j.envpol.2005.12.009

Carey SB, Jenkins J, Lovell JT et al (2020) The *Ceratodon purpureus* genome uncovers structurally complex, gene rich sex chromosomes. BioRxiv Prepr Serv Biol. https://doi.org/10.1101/2020.07.03.163634

Chen W, Taylor MC, Barrow RA et al (2019) Loss of phosphoethanolamine n-methyltransferases abolishes phosphatidylcholine synthesis and is lethal. Plant Physiol 179:124–142. https://doi.org/10.1104/pp.18.00694

Couée I, Sulmon C, Gouesbet G, El Amrani A (2006) Involvement of soluble sugars in reactive oxygen species balance and responses to oxidative stress in plants. J Exp Bot 57:449–459. https://doi.org/10.1093/jxb/erj027

Csupor D, Kurtán T, Vollár M et al (2020) Pigments of the moss *Paraleucobryum longifolium*: isolation and structure elucidation of prenyl-substituted 8,8′-linked 9,10-phenanthrenequinone dimers. J Nat Prod 83:268–276. https://doi.org/10.1021/acs.jnatprod.9b00655

Domingos M, Bulbovas P, Camargo CZS et al (2015) Searching for native tree species and respective potential biomarkers for future assessment of pollution effects on the highly diverse Atlantic Forest in SE-Brazil. Env Pollut 202:85–95. https://doi.org/10.1016/j.envpol.2015.03.018

Elkeilsh A, Awad YM, Soliman MH et al (2019) Exogenous application of β-sitosterol mediated growth and yield improvement in water-stressed wheat (*Triticum aestivum*) involves up-regulated antioxidant system. J Plant Res 132:881–901. https://doi.org/10.1007/s10265-019-01143-5

Erxleben A, Gessler A, Vervliet-Scheebaum M, Reski R (2012) Metabolite profiling of the moss *Physcomitrella patens* reveals evolutionary conservation of osmoprotective substances. Plant Cell Rep 31:427–436. https://doi.org/10.1007/s00299-011-1177-9

Esposito MP, Nakazato RK, Pedroso ANV et al (2018) Oxidant-antioxidant balance and tolerance against oxidative stress in pioneer and non-pioneer tree species from the remaining atlantic forest. Sci Total Env 625:382–393. https://doi.org/10.1016/j.scitotenv.2017.12.255

Fernández-Marín B, Kranner I, Sebastián MS et al (2013) Evidence for the absence of enzymatic reactions in the glassy state. a case study of xanthophyll cycle pigments in the desiccation-tolerant moss *Syntrichia ruralis*. J Exp Bot 64:3033–3043. https://doi.org/10.1093/jxb/ert145

Goss R, Wilhelm C (2009) Lipids in algae, lichens and mosses. In: Wada H, Murata N (eds) Lipids in photosynthesis: essential and regulatory functions. Springer Science, Dordrecht, pp 117–137

Goss R, Latowski D (2020) Lipid dependence of xanthophyll cycling in higher plants and algae. Front Plant Sci 11:455. https://doi.org/10.3389/fpls.2020.00455

Green TGA, Sancho LG, Pintado A (2011) Ecophysiology of desiccation/rehydration cycles in mosses and lichens. In: Lüttge U, Beck E, Bartels D (eds) Plant desiccation tolerance. Springer-Verlag, Berlin, Heidelberg, pp 89–120

Hallingbäck T, Hodgetts N. (2000) Mosses, liverworts, and hornworts Status survey and conservation action plan for Bryophytes IUCN/SSC Bryophyte Specialist Group IUCN Publications Services Unit, UK

Huang X, Xue J, Zhang J et al (2012) Effect of different wetness conditions on *Sphagnum* lipid composition in the erxianyan peatland, central China. Org Geochem 44:1–7. https://doi.org/10.1016/j.orggeochem.2011.12.005

Kessner D, Chambers M, Burke R et al (2008) Proteowizard: open source software for rapid proteomics tools development. Bioinformatics 24:2534–2536. https://doi.org/10.1093/bioinformatics/btn323

Klavina L. (2018) Composition of mosses, their metabolites and environmental stress impacts. Doctoral Thesis, University of Latvia

Latowski D, Kuczyńska P, Strzałka K (2011) Xanthophyll cycle—a mechanism protecting plants against oxidative stress. Redox Rep 16:78–90. https://doi.org/10.1179/174329211X13020951739938

Lee S, Suh S, Kim S et al (1997) Systemic elevation of phosphatidic acid and lysophospholipid levels in wounded plants. Plant J 12:547–558

Lenné T, Bryant G, Hocart CH et al (2010) Freeze avoidance: a dehydrating moss gathers no ice. Plant Cell Env 33:1731–1741. https://doi.org/10.1111/j.1365-3040.2010.02178.x

Li C, Liu S, Zhang W et al (2019) Transcriptional profiling and physiological analysis reveal the critical roles of ROS-scavenging system in the Antarctic moss *Pohlia nutans* under ultraviolet-B radiation. Plant Physiol Biochem 134:113–122. https://doi.org/10.1016/j.plaphy.2018.10.034

Lira BS, Gramegna G, Trench BA et al (2017) Manipulation of a senescence-associated gene improves fleshy fruit yield. Plant Physiol 175:77–91. https://doi.org/10.1104/pp.17.00452

Liu J, Moyankova D, Djilianov D, Deng X (2019) Common and specific mechanisms of desiccation tolerance in two gesneriaceae resurrection plants. Multiomics Evid Front Plant Sci 10:1067. https://doi.org/10.3389/fpls.2019.01067

Lu Y, Eiriksson FF, Thorsteinsdóttir M, Simonsen HT (2019) Valuable fatty acids in bryophytes production, biosynthesis, analysis and applications. Plants 8:524. https://doi.org/10.3390/plants8110524

McDaniel SF, Perroud PF, Cuming AC, Szövényi P (2016) The *Ceratodon purpureus* transcriptome ushers in the Era of moss comparative genomics. Adv Bot Res 78:141–166. https://doi.org/10.1016/bs.abr.2016.02.003

Nerlich A, Von Orlow M, Rontein D et al (2007) Deficiency in phosphatidylserine decarboxylase activity in the psd1 psd2 psd3 triple mutant of arabidopsis affects phosphatidylethanolamine accumulation in mitochondria. Plant Physiol 144:904–914. https://doi.org/10.1104/pp.107.095414

Oldenhof H, Wolkers WF, Bowman JL et al (2006) Freezing and desiccation tolerance in the moss *Physcomitrella patens*: an *in situ* Fourier transform infrared spectroscopic study. Biochim Biophys Acta—Gen Subj 1760:1226–1234. https://doi.org/10.1016/j.bbagen.2006.03.025

Oliver MJ, Tuba Z, Mishler BD et al (2000) The evolution of vegetative desiccation tolerance in land plants. Plant Ecol 151:85–100

Pejin B, Iodice C, Tommonaro G et al (2012) Sugar composition of the moss *Rhodobryum ontariense* (Kindb.) Kindb. Nat Prod Res 26:209–215. https://doi.org/10.1080/14786419.2010.535163

Pereira CS, Lins RD, Chandrasekhar I et al (2004) Interaction of the disaccharide trehalose with a phospholipid bilayer: a molecular dynamics study. Biophys J 86:2273–2285. https://doi.org/10.1016/S0006-3495(04)74285-X

Peters K, Worrich A, Weinhold A et al (2018) Current challenges in plant eco-metabolomics. Int J Mol Sci 19(5):1385. https://doi.org/10.3390/ijms19051385

Porembski S (2011) Evolution, diversity, and habitats of poikilohydrous vascular plants. In: Lüttge U, Beck E, Bartels D (eds) Plant desiccation tolerance ecological studies (analysis and synthesis), vol 215. Springer, Berlin, Heidelberg, pp 139–156. https://doi.org/10.1007/978-3-642-19106-0_8

Renault H, Alber A, Horst NA et al (2017) A phenol-enriched cuticle is ancestral to lignin evolution in land plants. Nat Commun 8:14713. https://doi.org/10.1038/ncomms14713

Sami F, Yusuf M, Faizan M et al (2016) Role of sugars under abiotic stress. Plant Physiol Biochem 109:54–61. https://doi.org/10.1016/j.plaphy.2016.09.005

Shepherd GJ (2010) FITOPAC 2.1. https://pedroeisenlohr.webnode.com.br/fitopac/. Accessed 01 Feb 2022

Smirnoff N (1992) The carbohydrates of bryophytes in relation to desiccation tolerance. J Bryol 17:185–191. https://doi.org/10.1179/jbr.1992.17.2.185

Sulamita D, Peralta DF, Silva AL, et al. (2021) Ditrichaceae in Flora do Brasil 2020 In: Flora do Brasil 2020. http://floradobrasil.jbrj.gov.br/reflora/floradobrasil/FB96231. Accessed 23 Sep 2021

Valli M, Russo HM, Pilon AC et al (2019) Computational methods for NMR and MS for structure elucidation II: database resources and advanced methods. Phys Sci Rev. https://doi.org/10.1515/psr-2018-0167

Wang M, Carver JJ, Phelan VV et al (2016) Sharing and community curation of mass spectrometry data with global natural products social molecular networking. Nat Biotechnol 34:828–837. https://doi.org/10.1038/nbt.3597

Waterman MJ, Nugraha AS, Hendra R et al (2017) Antarctic moss biflavonoids show high antioxidant and ultraviolet-screening activity. J Nat Prod 80:2224–2231. https://doi.org/10.1021/acs.jnatprod.7b00085

Williams B, Njaci I, Moghaddam L et al (2015) Trehalose accumulation triggers autophagy during plant desiccation. PLoS Genet 11:e1005705. https://doi.org/10.1371/journal.pgen.1005705